Journal of Medicinal Chemistry

pubs.acs.org/jmc Article

Discovery of EEDi-5273 as an Exceptionally Potent and Orally Efficacious EED Inhibitor Capable of Achieving Complete and Persistent Tumor Regression

Rohan Kalyan Rej,◆ Changwei Wang,◆ Jianfeng Lu, Mi Wang, Elyse Petrunak, Kaitlin P. Zawacki, Donna McEachern, Chao-Yie Yang, Lu Wang, Ruiting Li, Krishnapriya Chinnaswamy, Bo Wen,* Duxin Sun, Jeanne A. Stuckey, Yunlong Zhou, Jianyong Chen, Guozhi Tang, and Shaomeng Wang*

Cite This: J. Med. Chem. 2021, 64, 14540−14556 Read Online

ACCESS | Metrics & More | Article Recommendations | Supporting Information

ABSTRACT: Embryonic ectoderm development (EED) is a promising therapeutic target for human cancers and other diseases. We report herein the discovery of exceptionally potent and efficacious EED inhibitors. By conformational restriction of a previously reported EED inhibitor, we obtained a potent lead compound. Further optimization of the lead yielded exceptionally potent EED inhibitors. The best compound EEDi-5273 binds to EED with an IC_{50} value of 0.2 nM and inhibits the KARPAS422 cell growth with an IC_{50} value of 1.2 nM. It demonstrates an excellent PK and ADME profile, and its oral administration leads to complete and persistent tumor regression in the KARPAS422 xenograft model with no signs of toxicity. Co-crystal structures of two potent EED inhibitors with EED provide a solid structural basis for their high-affinity binding. EEDi-5273 is a promising EED inhibitor for further advanced preclinical development for the treatment of human cancer and other human diseases.

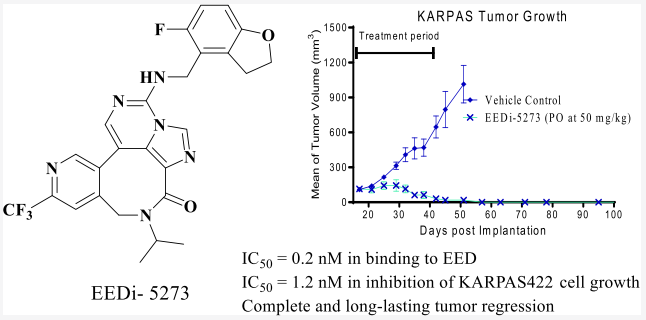

INTRODUCTION

The polycomb repressive complex 2 (PRC2) catalyzes trimethylation of histone H3 lysine 27 (H3K27), which is a repressive chromatin marker associated with gene silencing through chromatin compaction.[1,2] The human PRC2 consists of four core subunits, namely, enhancer of zeste homolog 2 [EZH2], embryonic ectoderm development [EED], suppressor of zeste 12 [SUZ12], and retinoblastoma suppressor associated protein 46/48 [RbAp46/48].[3] Although EZH2 is the main catalytic subunit of the PRC2 complex, EZH2 requires two other PRC2 components, EED and SUZ12, to be catalytically active. Of these components, EED holds both scaffolding and H3K27me3 binding functions. As a scaffolding protein, EED assembles and stabilizes the PRC2 complex and through its binding to H3K27me3, EED allosterically stimulates the catalytic activity of PRC2.[4,5]

Dysregulations in PRC2 have been found in a number of human cancers. For example, EZH2 mutations, including the single-point mutations Y641N and Y641F, occur in as many as 25% of diffuse large B-cell lymphomas (DLBCL) and follicular lymphomas (FL), and are associated with poor patient prognosis.[6−8] These mutations increase the trimethylase activity of the PRC2 complex, leading to increased levels of trimethylated lysine 27 (H3K27me3) in tumor cells and to aberrant gene expression.[9−11] Consequently, targeting the PRC2 catalytic activity is being pursued as a new cancer therapeutic strategy. In particular, intense research efforts have been made to discover and develop EZH2 inhibitors, a number of which have been advanced into clinical development (Figure 1).[12−15] Among them, Tazemetostat (**2**) was approved in 2020 by the US FDA for the treatment of advanced epithelioid sarcoma and follicular lymphoma (https://clinicaltrials.gov/ct2/show/NCT04204941), marking an important milestone in the development of EZH2 inhibitors for the treatment of human cancers (Figure 1).

Another alternative and attractive strategy to inhibit the PRC2 activity is to target EED. In 2017, scientists from Novartis and AbbVie reported their discovery of EED226 (**6**)[16] and A-395 (**7**),[17] respectively, as allosteric inhibitors of EED, which bind to the histone binding site in EED.[18−20] Subsequently, additional potent and efficacious EED inhibitors were reported, including BR-001 (**8**)[21] and EEDi-5285 (**9**),[22] from this laboratory. These EED inhibitors demonstrate

Received: June 12, 2021
Published: October 6, 2021

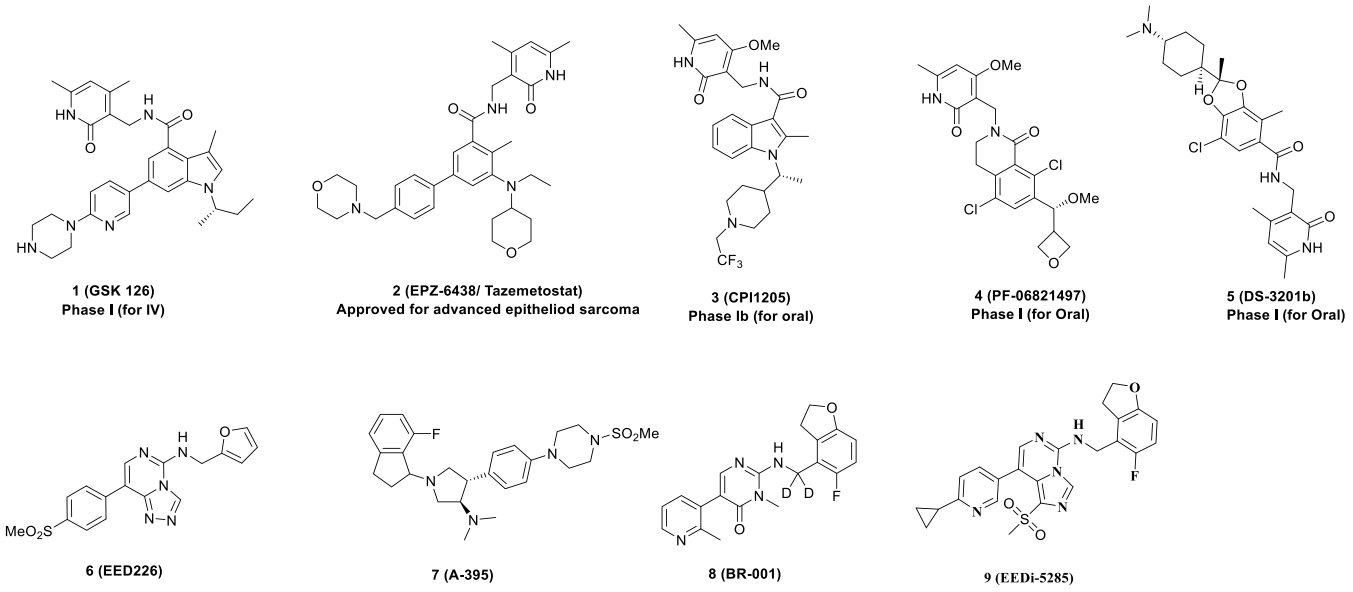

Figure 1. Representative small-molecule inhibitors of EZH2 and EED that target the PRC2 activity.

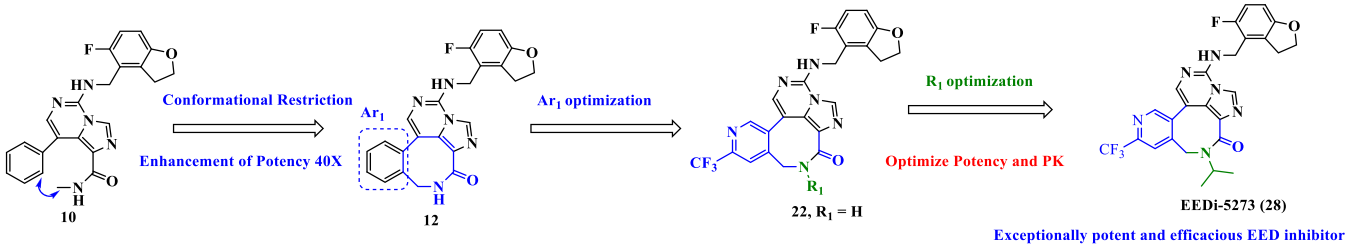

Figure 2. Structure-guided design and optimization of EED inhibitors.

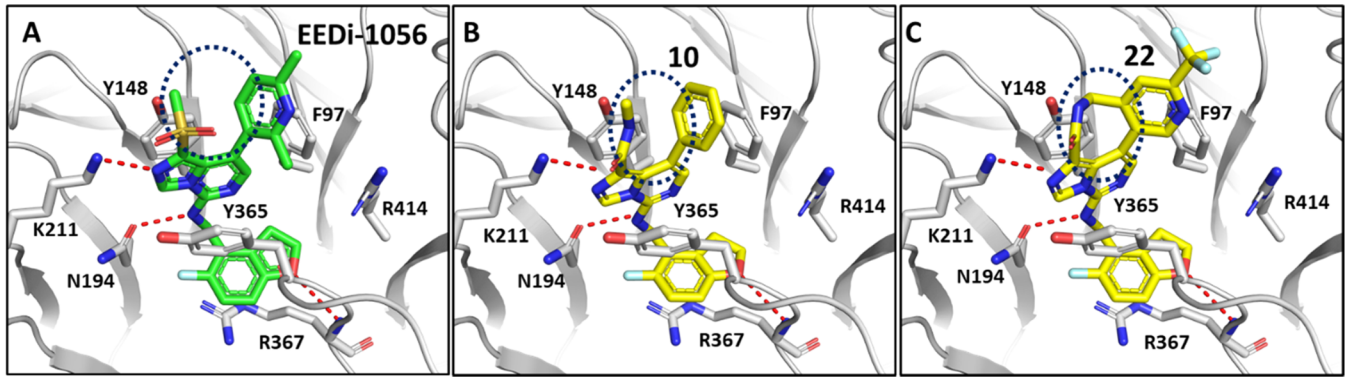

Figure 3. (A) Co-crystal structure of EED with EEDi-1056 (PDB accession code 6W7G) and predicted binding models of compounds (B) **10** and (C) **22** with EED. Dashed lines denote hydrogen bonds.

impressive antitumor activity in EZH2 mutant DLBCL models and were shown to be effective in a model resistant to EZH2 inhibitors, suggesting a potential advantage of EED inhibitors over EZH2 inhibitors. To date, only two EED inhibitors, MAK683 from Novartis (https://clinicaltrials.gov/ct2/show/NCT02900651) and FTX-6058 from Fulcrum Therapeutics (https://clinicaltrials.gov/ct2/show/NCT04586985), have progressed into clinical development.[23,24]

In the present study, we describe our structure-guided discovery of EEDi-5273 (**28**) as an exceptionally potent and orally active small-molecule inhibitor of EED, capable of achieving complete and long-lasting tumor regression.

RESULTS AND DISCUSSION

We used compound **10** (Figure 2), a previously disclosed EED inhibitor,[22] as the starting point for our design efforts based on the following considerations: (i) **10** has an excellent binding affinity to EED with IC_{50} = 19 nM and potent cell growth inhibitory activity with IC_{50} = 52 nM in the KARPAS422 cell line carrying a Y641N EZH2 mutation; (ii) **10** has favorable druglike properties; and (3) availability of co-crystal structures for structurally related EED inhibitors EED226 (PDB accession code 5GSA) and EEDi-1056 (PDB accession code 6W7G), which provide a structural basis for further structure-based optimization.

https://doi.org/10.1021/acs.jmedchem.1c01059
J. Med. Chem. 2021, 64, 14540−14556

We predicted the binding model of compound **10** in a complex with EED based on the co-crystal structures of EED226 and EEDi-1056 (Figure 3). Analysis of the predicted binding model for compound **10** suggested that its carboxamide group could be linked to the adjacent phenyl group in a cyclic structure. We hypothesized that proper cyclization may lock the phenyl group into its active conformation, thus reducing the conformational entropy loss upon binding to EED and leading to an improved binding affinity to EED.[25,26]

To test our hypothesis, we synthesized compounds **11**–**13** containing seven- to nine-membered lactam rings. These compounds were tested for their binding affinities to EED and their cell growth inhibitory activity in the KARPAS422 cell line carrying an EZH2 mutation. The data obtained are summarized in Table 1.

Table 1. Effect of Conformational Restriction on Cyclized Seven- to Nine-Membered-Ring Lactams

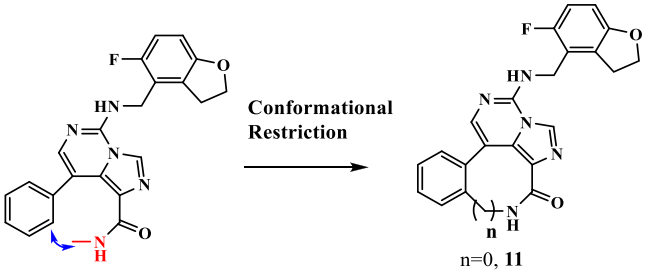

compd.	binding to EED (IC_{50}, nM)[a]	cell growth inhibition in KARPAS422 (IC_{50}, nM)[b]
10	18.8 ± 0.7	51.5 ± 0.7
11	19.5 ± 0.5	68.3 ± 0.4
12	0.5 ± 0.1	4.2 ± 0.6
13	13.8 ± 0.4	57.8 ± 0.9
EED226	12.2 ± 0.3	125.4 ± 13.4
A-395	4.8 ± 0.1	62.9 ± 5.4

[a]IC_{50} values were determined by an AlphaScreen assay; values reported are the mean ± SD of three experiments. [b]Cells were treated with compounds for 7 days, and cell growth was determined by a lactate dehydrogenase-based WST-8 assay.

Compound **11** with a seven-membered lactam ring and compound **13** with a nine-membered lactam ring have very similar binding affinities to EED compared to compound **10** (Table 1). Compounds **11** and **13** are consistently similarly potent in inhibition of cell growth in the KARPAS422 cell line compared to compound **10**. However, compound **12** containing an eight-membered lactam ring has an IC_{50} value of 0.5 nM in binding to EED and is 37 times more potent than compound **10**. Compound **12** achieves an IC_{50} value of 4.2 nM in inhibition of cell growth in the KARPAS422 cell line and is thus 12 times more potent than compound **10**. Hence, the binding affinity to EED and cell growth inhibitory activity in the KARPAS422 cell line for compound **12** are much improved over those of compound **10** and this supports our design strategy.

After successfully identifying compound **12** as a promising lead compound, we next focused our optimization efforts on the phenyl group and obtained the data summarized in Table 2. To improve the solubility of the compound, the phenyl

Table 2. Investigation of SAR on the Ar_1 Group

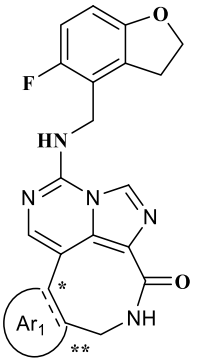

Compd.	Ar_1	Binding to EED (IC_{50}, nM)[a]	Cell growth inhibition in KARPAS422 cells (IC_{50}, nM)[b]
12		0.5±0.1	4.2±0.6
14		0.7±0.1	1.9±0.5
15		0.8±0.2	8.3±1.3
16		0.6±0.1	7.9±1.1
17		4.1±0.5	29.2±6.8
18		1.2±0.1	4.4±2.7
19		9.2±0.1	37.1±4.0
20		0.7±0.1	1.4±0.9
21		3.6±0.3	1.4±0.7
22		0.7±0.1	0.5±0.2
23		0.4±0.1	8.1±1.6
24		11.3±0.9	6.6±1.7
25		13.2±0.2	17.4±5.0

[a]a and b same as Table 1.

https://doi.org/10.1021/acs.jmedchem.1c01059
J. Med. Chem. 2021, 64, 14540−14556

group in **12** was replaced with pyridine, yielding compound **14**. Interestingly, while compound **14** is slightly less potent than **12** in binding to EED (IC_{50} = 0.5 vs 0.7 nM), it is twice as potent in inhibition of cell growth in the KARPAS422 cell line (IC_{50} = 4.2 vs 1.9 nM).

We investigated the effect of fluorine substitution at three different positions on the phenyl ring. Compound **15** with 1-F and compound **16** with 2-F are slightly less potent than compound **12** in binding to EED and are 2 times less potent than compound **12** in inhibition of cell growth in the KARPAS422 cell line. However, compound **17** with 3-F substitution is 7−8 times less potent than compound **12** both in binding to EED and in inhibition of KARPAS422 cell growth.

We investigated the effect of a CF_3 substituent at two different positions. Compound **18** with 2-CF_3 substitution is 2 times less potent than compound **12** in binding to EED but is equally potent as compound **12** in inhibition of KARPAS422 cell growth. However, compound **19** with 3-CF_3 substitution is 18 times less potent than compound **12** in binding to EED and 9 times less potent in inhibition of KARPAS422 cell growth.

Because of the high binding affinity to EED and the potent cell growth inhibition of compound **14**, we made further modifications to this compound, obtaining the data summarized in Table 2. Compound **20** containing a 2-methyl substituent is equipotent with compound **14** in both binding to EED and inhibition of KARPAS422 cell growth. Compound **21** containing a 2-CF_3−1-pyridine substitution is 5 times less potent than compound **14** in binding to EED but exhibits equal potency in inhibition of KARPAS422 cell growth. Compound **22** containing a 2-CF_3-3-pyridine group is equipotent with compound **12** in binding to EED, but it displays an IC_{50} value of 0.7 nM and is 8.4 times more potent than compound **12** in inhibition of KARPAS422 cell growth. Hence, compound **22** was identified as a very potent EED inhibitor.

Replacement of the phenyl group in **12** with a 1-methyl-1*H*-pyrazole led to compound **23**. Compound **23** has a similar binding affinity to EED as compound **12** (IC_{50} = 0.5 nM vs 0.4 nM), but it is 2 times less potent than compound **12** in inhibition of KARPAS422 cell growth (4.2 nM vs 8.1 nM). We synthesized compounds **24** and **25** by replacing the phenyl group with a thiophene but both compounds were found to be less potent than compound **12** in binding to EED and inhibition of KARPAS422 cell growth.

We assessed the oral exposure of five potent EED inhibitors in mice, and the data are summarized in Table 3. Disappointingly, all of these compounds had low or modest oral exposure in plasma.

We next focused our efforts on improving the oral bioavailability and overall pharmacokinetic profiles of our EED inhibitors. Based on its cell growth inhibition activity, compound **22** is a very potent EED inhibitor and accordingly, we performed further optimization of compound **22**.

Our predicted binding model for compound **22** suggests that the lactam group does not interact directly with EED. We proposed that N-alkylation of the amide linkage in compound **22** may improve its oral bioavailability because: (i) removal of a hydrogen bond donor reduces polar surface and (ii) change of the planar amide into a more twisted conformation can improve cell permeability and oral absorption. Accordingly, a series of N-alkylated analogues of compound **22** were synthesized and evaluated.

Table 3. Oral Exposure of EED Inhibitors in Plasma with a Single Oral Administration in Mice[a]

	plasma concentration (ng/mL) with a single PO administration at 25 mg/kg		
	time points		
Compound	1 h	3 h	6 h
12	110	100	<10
14	43	<10	<10
20	35	<10	<10
21	70	65	<10
22	90	170	95

[a]Each compound was administered orally at 25 mg/kg. Plasma samples were collected at 1, 3, and 6 h with two mice at each time point and analyzed by LC-MS/MS. Mean values of drug concentrations are presented.

We synthesized compounds **26**−**30** with an *N*-methyl, *N*-ethyl, *N*-isopropyl, *N*-cyclopropyl, and *N*-cyclobutyl substituent, respectively (Table 4). Compound **26** with an *N*-methyl substitution binds to EED with an IC_{50} value of 0.6 nM and achieves an IC_{50} value of 0.9 nM in inhibition of KARPAS422 cell growth, and thus is as potent as **22**. Compound **27** with an *N*-ethyl substitution has a binding affinity and cell growth inhibitory activity very similar to that of **26**. Compound **28** (EEDi-5273) with an *N*-isopropyl group binds to EED with an IC_{50} value of 0.2 nM and inhibits KARPAS422 cell growth with IC_{50} = 1.2 nM. Compound **29** with an *N*-cyclopropyl group binds to EED with an IC_{50} value of 1.5 nM and has an IC_{50} value of 1.3 nM in inhibition of KARPAS422 cell growth. Compound **30** with an N-cyclobutyl group binds to EED with an IC_{50} value of 0.8 nM and has an IC_{50} value of 2.0 nM in inhibition of KARPAS422 cell growth.

We next synthesized and evaluated compounds **31**−**34** containing a fluorinated *N*-alkyl group. Compounds **31**−**34** bind to EED with IC_{50} values of 0.8−3.2 nM and inhibit KARPAS422 cell growth with IC_{50} values of 1.2−2.2 nM.

To improve the physicochemical properties of the compounds, we synthesized **35**−**42** containing different *N*-substituted hydrophilic groups. Compounds **35**−**42** are all high-affinity EED inhibitors with IC_{50} values of 0.6−1.8 nM. Consistent with their high binding affinities to EED, all of these compounds, with the exception of compound **41**, display a single-digit nM IC_{50} value in inhibition of KARPAS422 cell growth (Table 4).

Evaluation of Oral Exposure in Mice. We selected a total of 12 potent EED inhibitors and evaluated their oral plasma exposures in mice. The resulting data are summarized in Table 5.

These exposure data showed that among these 12 compounds, compounds **28**, **29**, **31**, and **32** achieve high oral exposure, while compounds **26**, **34**, **36**, and **37** show modest oral exposure. Compounds **39**, **40**, **41**, and **42** containing N-substituted hydrophilic groups all display low oral exposure.

Based on these initial oral exposure data, we selected compounds **28**, **31**, and **32** for full pharmacokinetic studies in mice with both intravenous and oral routes of administration and obtained the data summarized in Table 6.

With intravenous administration of 2 mg/kg, compounds **28**, **31**, and **32** all have low clearance and achieve high exposures but display modest volume of distribution. Compounds **28**, **31**, and **32** all achieve excellent oral

https://doi.org/10.1021/acs.jmedchem.1c01059
J. Med. Chem. 2021, 64, 14540−14556

Table 4. Representative Example of a Substituted Eight-Membered-Ring Lactams Containing Both a Hydrophobic and a Hydrophilic Tail as the R_1 Substituent

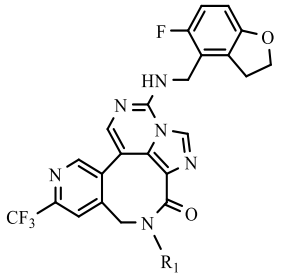

Compd.	R_1	Binding to EED (IC_{50}, nM)[a]	Cell growth inhibition in KARPAS422 cells (IC_{50}, nM)[b]
26		0.6 ± 0.1	0.9 ± 0.1
27		0.6 ± 0.1	1.0 ± 0.4
28		0.2 ± 0.1	1.2 ± 0.7
29		1.5 ± 0.1	1.3 ± 0.6
30		0.8 ± 0.1	2.0 ± 0.6
31		1.6 ± 0.1	1.2 ± 0.2
32		1.4 ± 0.4	1.2 ± 0.2
33		3.2 ± 0.1	1.9 ± 0.3
34		0.8 ± 0.2	2.2 ± 0.5
35		1.6 ± 0.1	4.6 ± 0.3
36		0.7 ± 0.1	1.0 ± 0.1
37		1.0 ± 0.1	3.9 ± 0.1
38		1.1 ± 0.1	1.5 ± 0.1
39		1.8 ± 0.1	6.3 ± 0.7
40		0.6 ± 0.1	3.1 ± 0.7
41	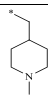	1.0 ± 0.1	14.9 ± 3.3
42		1.6 ± 0.1	2.4 ± 0.6
EED226		12.2 ± 0.3	125.4±13.4
A-395		4.8 ± 0.1	62.9±5.4

[a]a and b same as Table 1.

Table 5. Oral Exposure of EED Inhibitors in Plasma with Oral Administration in Mice[a]

	plasma drug concentration (ng/mL), PO (25 mg/kg)		
	time points		
compd.	1 h	3 h	6 h
26	226	216	87
28	12 780	3126	793
29	4895	3570	503
31	16 020	6190	11 650
32	4485	9165	4030
34	644	646	379
36	197	145	<10
37	157	125	259
39	60	30	9
40	70	45	51
41	<10	<10	<10
42	20	16	<10

[a]Each compound was administered orally at 25 mg/kg. Plasma samples were collected at 1, 3, and 6 h from two mice at each time point and analyzed by LC-MS/MS. Mean values of drug concentrations are presented.

bioavailability with AUC values of 48.9, 265.2, and 370.5 h·μg/mL, respectively, with 10 mg/kg PO administration and have an absolute oral bioavailability of 43, 88, and 90%, respectively.

Evaluation of microsomal stability showed that compound **28**, with $T_{1/2}$ > 120 min has excellent human microsomal stability but only moderate microsomal stability in rat and mouse species ($T_{1/2}$ = 87 and 67 min, respectively). Both compounds **31** and **32** have moderate microsomal stability in human and rat species and excellent microsomal stability in mice.

Importantly, none of these three compounds show inhibition of hERG. CYP testing showed that these three compounds fail to inhibit CYP3A2, CYP1A4, and CYP2B6 up to 30 μM and are weak inhibitors of CYP2C9, CYP2C19, and CYP2D6. Furthermore, these three compounds showed no CYP induction at 10 μM.

We next evaluated the plasma protein binding (PPB) with the data shown in Table 6. Among them, compound **28** has the best PPB profile with 98, 99, and 99% of PPB in human, rat, and mouse plasma, respectively. In comparison, both compounds **31** and **32** display >99% of PPB in human, rat, and mouse plasma. Hence, compound **28** has a major PPB advantage over compounds **31** and **32**.

Determination of Co-crystal Structures of Two Potent EED Inhibitors Complexed with EED. We determined co-crystal structures of **18** and **32** in complexes with EED (PDB accession code 7MSB and 7MSD, respectively). These co-crystal structures (Figure 4) show that for both compounds, the 5-fluoro-2,3-dihydrobenzofuran group fills the space in the deep pocket of EED, excludes interacting water molecules present in the EED226 structure (Figure 4C) and engages in cation−π interactions with the guanidinium group of Arg367 of EED. Such a hand-in-glove fit naturally creates more van der Waals interactions with EED than the furan group in EED226 as demonstrated by Tyr365. The side chain of Tyr365 is directly above the benzene ring of the 5-fluoro-2,3-dihydrobenzofuran group and induces π-π interactions, while the backbone Cα and the carbonyl group lie flat above the furan group increasing the van der Waals interactions. The electron-deficient bicyclic imidazo[1,5-*c*]-

https://doi.org/10.1021/acs.jmedchem.1c01059
J. Med. Chem. 2021, 64, 14540−14556

Table 6. Profiles of 28 (EEDi-5273), 31, and 32[a,b]

compd.	28 (EEDi-5273)	31	32
	PO PK Parameters at 10 mg/kg in Mice		
$T_{1/2}$ (h)	2.4	4.4	5.5
C_{max} (μg/mL)	5.07	20.3	24.4
AUC (h·μg/mL)	48.9	265.2	370.5
F (%)	43	88	90
	IV PK Parameters at 2 mg/kg		
AUC (h·μg/mL)	19.6	58.1	81.2
Cl (mL/min/kg)	1.71	0.59	0.39
V_{ss} (L/kg)	0.36	0.22	0.18
	Liver Microsomal Stability		
$t_{1/2}$ (min) H/R/M	>120/87/ 67	35/40/>120	46/53/>120
Cl_{int} (mL/min/kg) H/R/M	5.65/18.9/42.9	11.4/20.0/<16.6	9.9 /16.6/<12.4
	CYP Inhibition % Inhibition IC_{50} (μM)		
CYP1A2, CYP2B6, CYP2C9, CYP2C19, CYP2D6, and CYP3A4	>30, >30, 8.8, 17.9, 14.3, >30	>30, >30, 7.8, 4.8, 18.9, >30	>30, >30, 7.3, 13.2, 19.7, >30
CYP induction	no induction to CYP1A2, CYP2B6, CYP3A4 at 10 μM	no induction to CYP1A2, CYP2B6, CYP3A4 at 10 μM	no induction to CYP1A2, CYP2B6, CYP3A4 at 10 μM
hERG IC_{50} (μM)	>30	>30	>30
plasma stability $t_{1/2}$ (H/D/R/M, min)	>120	>120	>120
PPB (F bound%) H/R/M	98/ 99/99	>99	>99

[a]Dose-normalized total exposure following IV dosing of 2 mg/kg in male CD-1 mice; formulated in 10% dimethyl sulfoxide (DMSO), 5% Solutol HS15, and 85% Saline. Dose-normalized total exposure following oral (PO) dosing of 10 mg/kg in male CD-1 mice; formulated in 20% DMSO, 10% Solutol HS15, and 70% Distilled water. [b]Abbreviations: Cl = plasma clearance, V_{ss} = volume of distribution, $t_{1/2}$ = terminal half-life, F = oral bioavailability, CYP, cytochrome P450, (H/D/R/M = human/dog/rat/mouse), PPB = plasma protein binding.

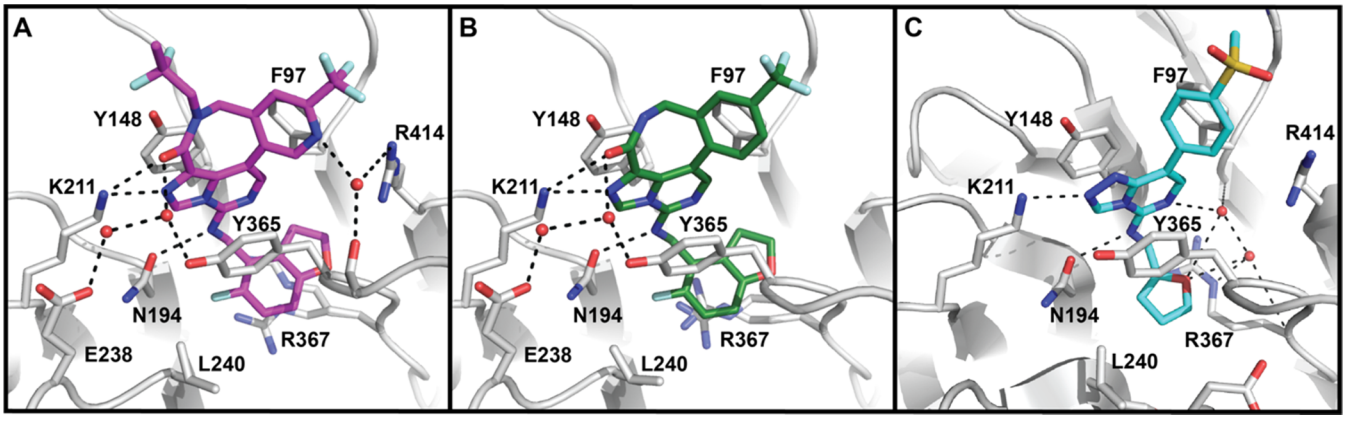

Figure 4. Co-crystal structures of EED inhibitors **18** and **32** in complex with EED. Key interactions of compounds (A) **32** with EED (PDB accession code 7MSD), (B) **18** with EED (PDB accession code 7MSB), and (C) EED226 with EED (PDB accession code 5GSA) are shown for comparison. Dashed lines represent hydrogen bonds. Water molecules are depicted as red spheres.

pyrimidine core forms $\pi-\pi$ stacking interactions with the electron-rich Tyr148 and Tyr365 residues of EED. Both the compound-protein structures are also stabilized by three hydrogen bond interactions. The amino group linking with the bicyclic imidazo pyrimidine core forms a hydrogen bond with the side-chain carbonyl oxygen of Asn194, and the lower nitrogen of the imidazo pyrimidine core and carboxamide group form two hydrogens bonds with the side chain amine of Lys211. The substituted phenyl group undergoes an edge-to-face interaction with the side chain of Phe97, and the 2,2-difluoropropane substituent in compound **32** fails to show any additional interaction as it is outside the binding pocket. These two co-crystal structures provide a solid structural basis for the very high affinities of compounds **18** and **32** with EED (Figure 4).

Antitumor Activity of Compound 28 (EEDi-5273) in the KARPAS422 Xenograft Model. Based upon its overall excellent PK and ADME profile and exceptional potency in binding to EED and in inhibition of KARPAS422 cell growth, we evaluated compound **28** (EEDi-5273) for its antitumor activity in the KARPAS422 xenograft model in mice, with the data summarized in Figure 5.

When tumors grew to an average volume of approximately 110 mm^3, the mice were treated with EEDi-5273 at either 50 or 75 mg/kg daily for 5 weeks or vehicle control *via* oral gavage. Our data showed that EEDi-5273 at both 50 mg and 75 mg/kg achieved complete tumor regression during the treatment period (days 17−51). To investigate if the tumor regression was persistent, we monitored the tumor growth for an additional 71 days after the last dose (Figure 5A). For the group treated with EEDi-5273 at 50 mg/kg, one out of five tumors regrew on day 114 and the second tumor regrew on day 122. For the group treated with EEDi-5273 at 75 mg/kg, one out of five tumors regrew on day 78 and all other four

https://doi.org/10.1021/acs.jmedchem.1c01059
J. Med. Chem. 2021, 64, 14540−14556

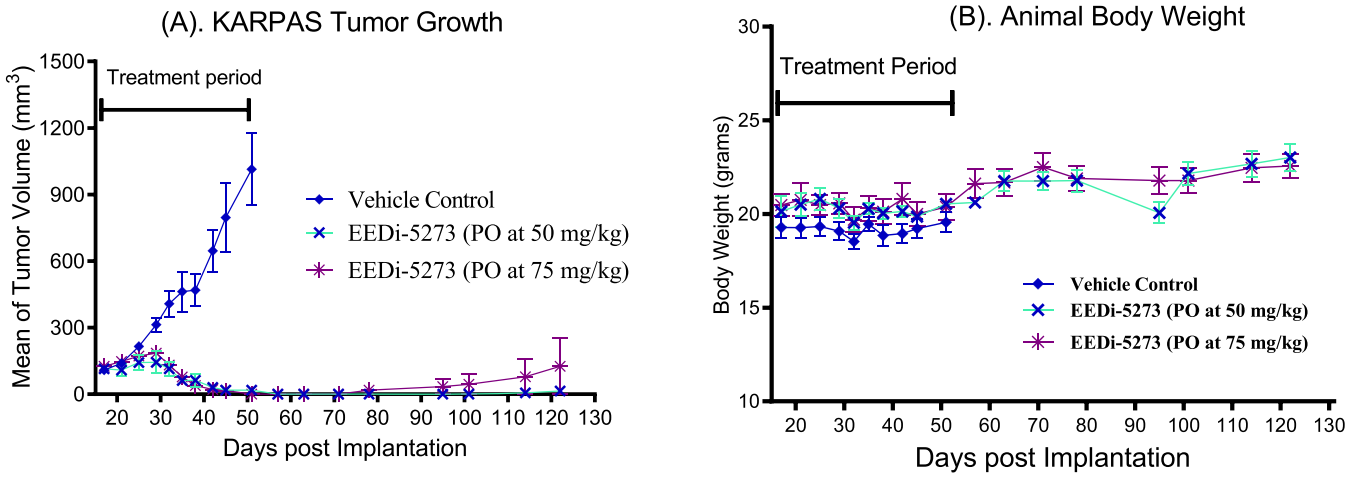

Figure 5. (A) Antitumor activity of EEDi-5273 in KARPAS422 xenograft model in severe combined immune-deficient (SCID) mice. Each group had five mice, and each mouse had one tumor. (B) Changes in animal body weights.

Scheme 1. Synthetic Route to the Common Intermediate (48)[a]

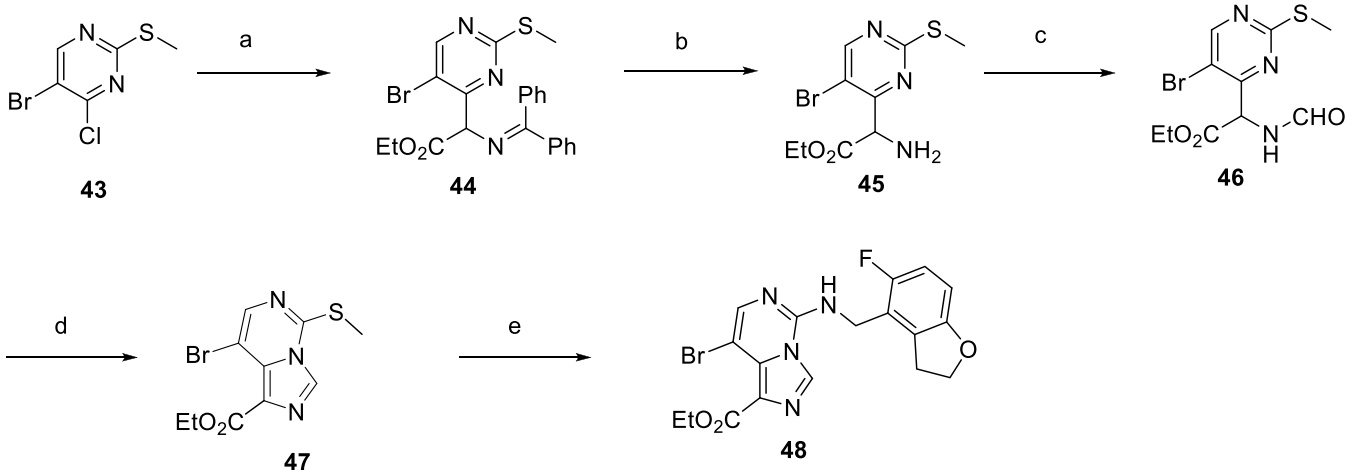

[a]Reagents and conditions: (a) ethyl 2-(diphenylmethyleneamino)acetate, NaH, rt, 2 h; (b) 3 N HCl in THF, rt, 1 h, 70%; (c) HCO_2H, Ac_2O, 50 °C, 2 h; (d) $POCl_3$, dioxane, reflux, 4 h, 70%; (e) (i) 1.5 equiv, mCPBA, 45 min, dichloromethane (DCM); (ii) 5-fluoro-2,3-dihydrobenzofuran-4-yl methanamine, rt, 3 h, 55%.

Scheme 2. Synthesis of (5-Fluoro-2,3-dihydrobenzofuran-4-yl)methanamine (56)[a]

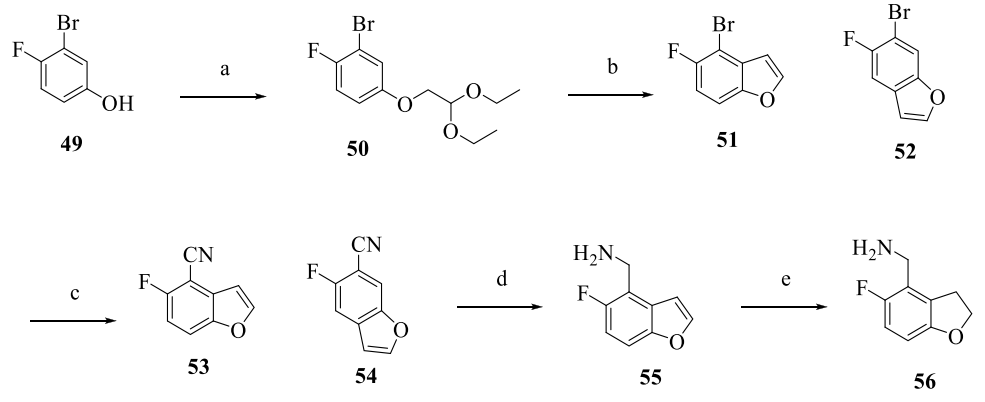

[a]Reagents and conditions: (a) 2-bromo-1,1-diethoxyethane, K_2CO_3, *N*,*N*-dimethylformamide (DMF), 110 °C, overnight, 75%; (b) polyphosphoric acid (PPA), toluene, 100 °C, 4 h, 55%; (c) $Zn(CN)_2$, $Pd(PPh_3)_4$, DMF, 110 °C, 24 h, 40%; (d) LAH, THF, 50 °C, 70%; (e) H_2, Pd/C, 40 °C, 6 h, 85%.

animals remained tumor-free during the entire experiment. Hence, EEDi-5273 is capable of achieving long-lasting and

https://doi.org/10.1021/acs.jmedchem.1c01059
J. Med. Chem. 2021, 64, 14540−14556

Scheme 3. General Procedure for Seven-, Eight-, or Nine-Membered Lactam Rings (11, 12, and 13 as Examples)[a]

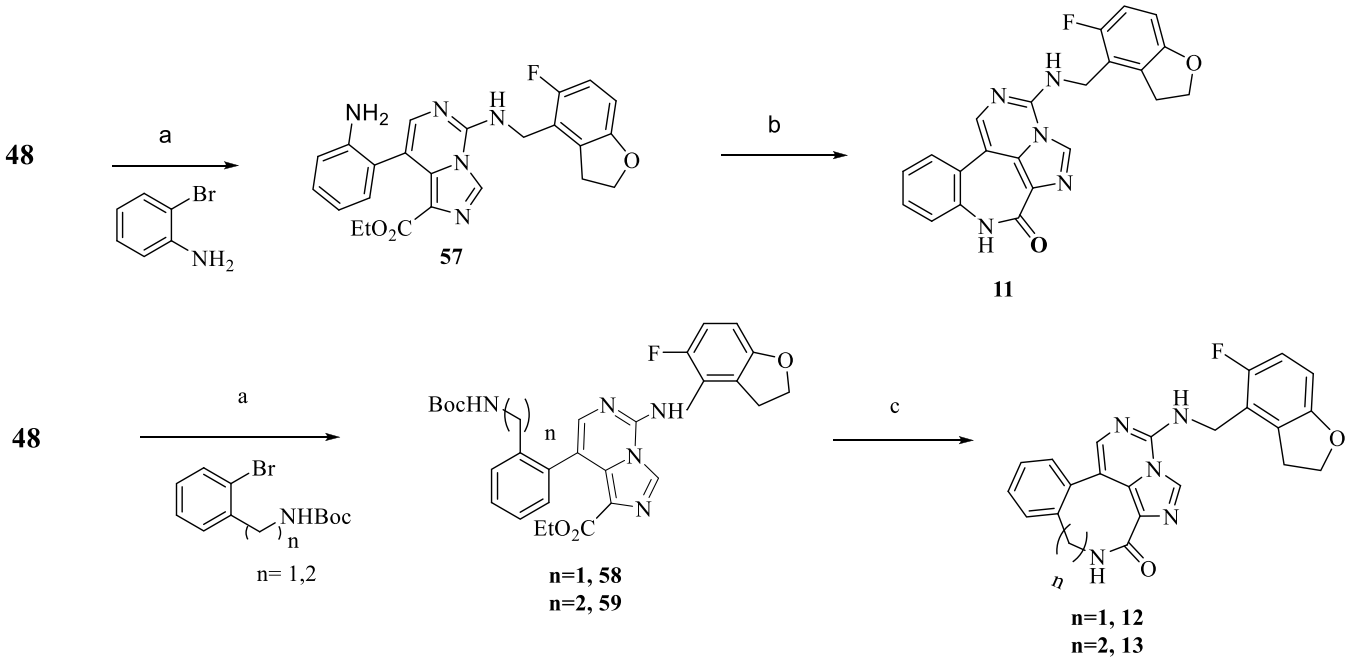

[a]Reagents and conditions: (a) $Pd(OAc)_2$, CataCXium A, K_2CO_3, bis(pinacolato)diboron, DME, 80 °C, ~50−60%; (b) $Li(OH)_2$, THF-H_2O, 70 °C, 90%; (c) (i) TFA, DCM, (ii) $Li(OH)_2$, THF-H_2O, 70 °C, 90%.

Scheme 4. General Procedure for Substituted Eight-Membered-Ring Lactams Containing Both Hydrophobic and Hydrophilic Tail as R_1 Substituent (28 as an Example)[a]

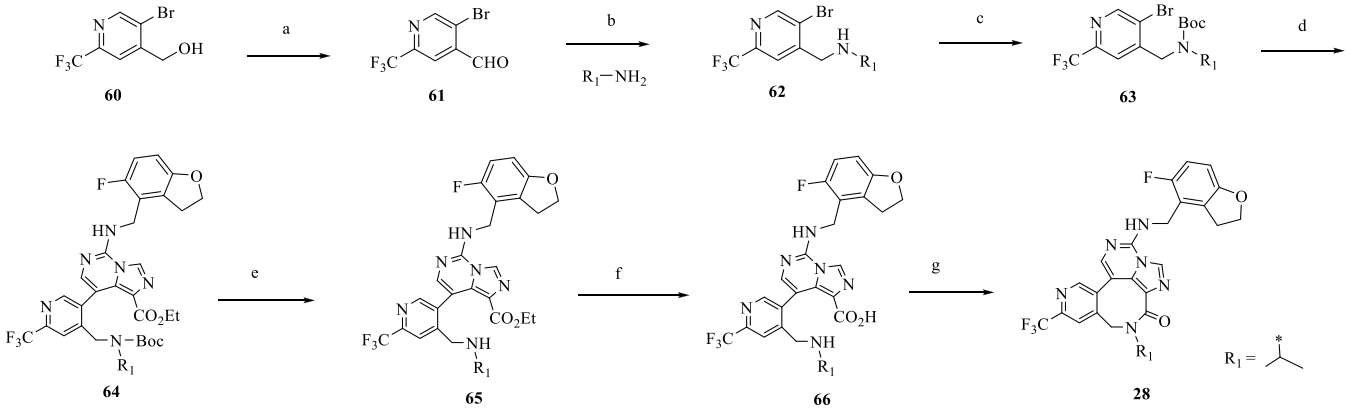

[a]Reagents and conditions: (a) DMP, DCM, rt, 2 h, 90%; (b) MeOH, $NaCNBH_3$, 3 h, R_4-NH_2, ~70%; (c) $(Boc)_2O$, Et_3N, DCM, 1 h, 90%; (d) **48**, $Pd(OAc)_2$, CataCXium A, K_2CO_3, bis(pinacolato)diboron, DME, 80 °C, overnight, ~50−60%; (e) TFA, DCM; (f) $Li(OH)_2$, THF-H_2O, 70 °C, overnight, 90%; (g) HATU, *N*,*N*-diisopropylethylamine (DIPEA), DMF, 90%.

complete tumor regression. Significantly, it did not cause animal weight loss or other signs of toxicity during the entire experiment (Figure 5B).

Chemistry. The synthesis of our designed EED inhibitors employed a common intermediate (**48**), which was prepared as outlined in Scheme 1. A second common intermediate, 5-fluoro-2,3-dihydrobenzofuran-4-yl methanamine (**56**) was prepared as shown in Scheme 2. Compounds **11**−**25** were prepared as shown in Scheme 3, and compounds **26**−**42** were prepared as shown in Scheme 4.

The route to the common intermediate **48** began with commercially available 5-bromo-4-chloro-2-(methylthio)-pyrimidine (**43**), which was converted to the corresponding amine (**45**) by treatment with ethyl 2-(diphenylmethyleneamino)acetate, followed by acid-catalyzed hydrolysis. The amine (**46**) upon formylation followed by cyclization using $POCl_3$ afforded compound **45**. Compound **47** was then oxidized to the corresponding sulfoxide intermediate by mCPBA, which was subsequently converted to the common intermediate **48** by selective displacement with 5-fluoro-2,3-dihydrobenzofuran-4-yl methanamine at the 5-position in 55% overall yield in two steps.[22,27,28]

The synthesis of 5-fluoro-2,3-dihydrobenzofuran-4-yl methanamine (**56**) is shown in Scheme 2.[22,29] Commercially available compound **49** was alkylated with 2-bromo-1,1-diethoxyethane using K_2CO_3 as a base and underwent cyclization in the presence of PPA affording two inseparable isomers **51** and **52** in a 1:1 mixture. The mixture was then treated with $Zn(CN)_2$ in the presence of $Pd(PPh_3)_4$ to furnish isomeric compounds **53** and **54** and the desired isomer **53** was

https://doi.org/10.1021/acs.jmedchem.1c01059
J. Med. Chem. 2021, 64, 14540−14556

isolated and obtained in 40% yield. Reduction of the nitrile functionality using LAH yielded compound **55**, which on hydrogenation using Pd/C furnished the desired amine **56**.

The general synthesis of compounds with seven-, eight-, or nine-membered lactam rings is shown in Scheme 3. The modified Suzuki reaction[30] between compound **48** and the appropriate bromo precursor proceeded smoothly in the presence of $Pd(OAc)_2$, cataCXium A, bis(pinacolato)diboron and yielded compounds in 50−60% yield. For seven-membered lactam rings, the free amine and ester group underwent cyclization using LiOH as a base. For eight- or nine-membered lactam rings, the target compounds were obtained by a two-step protocol, first deprotection of Boc group using TFA, followed by cyclization using LiOH as a base.

General synthesis of the substituted eight-membered-ring lactams is depicted in Scheme 4. This general synthesis allows efficient modification of the amide region of the molecule. The synthesis started with a commercially available alcohol (**60**) which on subsequent DMP oxidation, followed by reductive amination afforded the desired amine. Boc protection of the amine functionality in compound **62** was achieved by treatment with $(Boc)_2O$ in the presence of Et_3N. The modified Suzuki cross-coupling reaction between compound **48** and appropriate bromo precursor (**63**) in the presence of $Pd(OAc)_2$, CataCXium A, and bis(pinacolato)diboron yielded compounds in 50−60% yield. TFA deprotection of Boc functionality followed by ester hydrolysis using LiOH yielded the desired target compound **66**. Compound **66** in the presence of HATU underwent intramolecular cyclization to furnish the desired substituted eight-membered-ring lactams in a 90% yield.

DISCUSSION AND CONCLUSIONS

Through conformational restriction and systematic structure−activity relationship studies, we have obtained a new class of exceptionally potent and orally bioavailable EED inhibitors, with EEDi-5273 (**28**) identified as the most promising compound. EEDi-5273 binds to EED with an IC_{50} value of 0.2 nM and is 24 and 61 times more potent than A-395 and EED226, respectively. EEDi-5273 potently inhibits the KARPAS422 cell growth with an IC_{50} value of 1.2 nM and is 52 and 104 times more potent than A-395 and EED226, respectively. EEDi-5273 has an excellent PK and ADME profile, and oral administration of EEDi-5273 is capable of achieving complete and persistent tumor regression in the KARPAS422 xenograft model without causing any signs of toxicity. Determination of two co-crystal structures of two highly potent EED inhibitors in a complex with EED provides a solid structural basis for their exceptionally high binding affinities to EED.

We have previously reported the discovery of EEDi-5285 as an exceptionally potent and efficacious EED inhibitor.[22] While EEDi-5285 and EEDi-5273 are similarly potent and efficacious *in vitro* and *in vivo*, EEDi-5273 has a much better oral exposure than EEDi-5285 based on their PK data. At 10 mg/kg oral administration, EEDi-5285 shows a cMax of 1.8 μg/mL (3.7 μM) and an AUC value of 6.0 h·μg/mL.[22] In comparison, at the same dose and using the same formulation, EEDi-5273 achieves a cMax of 5.07 μg/mL (9.63 μM) and an AUC value of 48.9 h·μg/mL. Hence, EEDi-5273 achieves 2.6-fold higher cMax and 8.2-fold higher AUC than EEDi-5285, respectively. To understand the much improved oral exposure for EEDi-5273 over EEDi-5285, we determined their solubility in fasted state simulated intestinal fluid (FaSSIF) and fed state simulated intestinal fluid (FeSSIF). It was found that EEDi-5285 has a very low solubility in FaSSIF (0.0265 mg/mL) and an extremely low solubility in FeSSIF (<0.001 mg/mL). In comparison, EEDi-5285 has a solubility of 3.11 mg/mL in FaSSIF and 0.44 mg/mL in FeSSIF. Hence, EEDi-5273 has >100 times improved solubility than EEDi-5285 in both FaSSIF and FeSSIF, which is consistent with its much higher oral exposure. Since we are interested in development of an orally bioavailable EED inhibitor as a new therapy for the treatment of human cancers and other human diseases, EEDi-5273 thus has a significant advantage over EEDi-5285 due to the much improved solubility in both FaSSIF and FeSSIF.

Collectively, our data show that EEDi-5273 represents a highly promising EED inhibitor for further advanced preclinical development for the treatment of human lymphoma and other types of human cancer in which the PRC2 complex activity may play a key role.

EXPERIMENTAL SECTION

General Information. Unless otherwise specified, all commercial reagents were used as supplied without further purification, and all reactions were performed under a nitrogen atmosphere in a dry solvent under anhydrous conditions. NMR spectra were obtained on a Bruker 400 Ascend spectrometer at a ^1H frequency of 400 MHz and a ^{13}C frequency of 100 MHz. Chemical shifts (δ) are reported in parts per million (ppm) relative to an internal standard. The final products were purified on a preparative high-performance liquid chromatography (HPLC) column (Waters 2545, Quaternary Gradient Module) with a SunFire Prep C18 OBD 5 μm 50 × 100 mm^2 reversed-phase column. The mobile phase was a gradient of solvent A (H_2O with 0.1% TFA) and solvent B (CH_3CN with 0.1% of TFA) at a flow rate of 60 mL/min and 1%/min increase of solvent B. All final compounds have purity ≥95% as determined by Waters ACQUITY ultra-performance liquid chromatograph (UPLC) using reversed-phase column (SunFire, C18, 5 μm, 4.6 × 150 mm^2) and a solvent gradient of A (H_2O with 0.1% of TFA) and solvent B (CH_3CN with 0.1% of TFA). Electrospray ionization (ESI) mass spectral (MS) analysis was performed on a Thermo Scientific LCQ Fleet mass spectrometer.

*Ethyl 2-(5-bromo-2-(methylthio)pyrimidin-4-yl)-2-((diphenylmethylene)amino)acetate (**44**).* A solution of ethyl 2-(diphenylmethyleneamino)acetate (18.4 g, 69 mmol) in DMSO (50 mL) was added dropwise at 0 °C to a suspension of 60% NaH (5.0 g, 125.5 mmol) in anhydrous DMSO (70 mL). The reaction mixture turned orange immediately. After 5 min, 5-bromo-4-chloro-2-(methylthio)pyrimidine (**43**, 15 g, 62.7 mmol) in 50 mL of DMSO was added dropwise. The mixture was then stirred at room temperature (rt) for 2 h. Then, the reaction mixture was quenched by careful addition of aq. NH_4Cl solution. The mixture was extracted with EtOAc, washed with brine, dried, concentrated, and used in the next step as obtained. LC-MS: $[M + H]^+$ = 470.01

*Ethyl 2-Amino-2-(5-bromo-2-(methylthio)pyrimidin-4-yl)acetate (**45**).* 3 N HCl in H_2O (10 mL) was added at 0 °C to a solution of crude compound **44** (5.0 g, 10.6 mmol) in THF (50 mL). The mixture was stirred at rt for 1 h, and the reaction mixture was then concentrated followed by adjustment of the pH to 8−9 with aq. Na_2CO_3 solution. The mixture was extracted with DCM and washed with brine. Concentration under reduced pressure followed by purification by flash chromatography (0−100% EtOAc/hexane) gave the desired compound **45** (2.26 g) in 70% overall yield. ^1H NMR (400 MHz, $CDCl_3$) δ 8.58 (s, 1H), 4.99 (s, 1H), 4.26−4.16 (m, 2H), 2.53 (s, 3H), 1.26 (t, 3H). LC-MS: $[M + H]^+$ = 305.95

*Ethyl 2-(5-Bromo-2-(methylthio)pyrimidin-4-yl)-2-formamidoacetate (**46**).* A mixture of HCO_2H (4 mL) and Ac_2O (4 mL) was heated at 50 °C for 1 h. The reaction mixture was cooled to rt and added to a solution of compound **45** (2.0 g, 6.55 mmol) in DCM (20 mL). The mixture was stirred at rt for 2 h and then concentrated. The

https://doi.org/10.1021/acs.jmedchem.1c01059
J. Med. Chem. 2021, 64, 14540−14556

mixture was extracted with DCM (2 × 50 mL) and washed successively with H_2O (20 mL) and brine (10 mL). The organic phase was dried over Na_2SO_4, filtered, and concentrated to afford the crude title compound **46** as an oil, which was used in the next steps without further purification. ^{1}H NMR (400 MHz, $CDCl_3$) δ 8.63 (s, 1H), 8.32 (s, 1H), 7.02 (brs, 1H), 6.20 (d, 1H), 4.31-4.11 (m, 2H), 2.54 (s, 3H), 1.27 (t, 3H). LC-MS: $[M + H]^+$ = 334.05

*Ethyl 8-Bromo-5-(methylthio)imidazo[1,5-c]pyrimidine-1-carboxylate (**47**).* $POCl_3$ (1.5 mL) was added dropwise to a solution of compound **46** (2.0 g, crude) in dioxane (20 mL). The reaction mixture was heated under reflux for 4 h. The mixture was cooled to rt then concentrated. Ice/H_2O (50 mL) was added, and the mixture was adjusted to pH 8 with satd. aq. $NaHCO_3$. The mixture was extracted with DCM (2 ×50 mL), washed with brine (10 mL), dried over Na_2SO_4, and filtered. The filtrate was concentrated, and the residue was purified by silica gel column chromatography (eluting with 50−100% EtOAc/hexane) to afford the title compound (**47**) as a white solid (1.42 g, 4.59 mmol) in 70% overall yield over two steps. ^{1}H NMR (400 MHz, DMSO-d_6): 8.65 (s, 1H), 7.97 (s, 1H), 4.33 (q, 2H), 2.76 (s, 3H), 1.34 (t, 3H). ^{13}C NMR (100 MHz, DMSO-d_6) δ 162.33, 149.30, 139.51, 129.49, 128.44, 125.00, 103.79, 61.02, 14.65, 13.94. LC-MS: $[M + H]^+$ = 315.70

*Ethyl 8-Bromo-5-(((5-fluoro-2,3-dihydrobenzofuran-4-yl)-methyl)amino)imidazo[1,5-c]pyrimidine-1-carboxylate (**48**).* mCPBA (464 mg, 2.7 mmol, ≤77%, 1.5 equiv) was added at 0 °C to a solution of compound **47** (567 mg, 1.8 mmol, 1.0 equiv) in DCM (18 mL). After 45 min, Et_3N (1 mL, 7.6 mmol, 4 equiv) was added at 0 °C and stirred for 2 min, followed by addition of (5-fluoro-2,3-dihydrobenzofuran-4-yl)methanamine (300 mg, 1.8 mmol). The reaction mixture was then stirred at rt for 3 h. Subsequently, the reaction mixture was concentrated and the residue was purified by silica gel column chromatography (eluted with 50−100% EtOAc/hexane) to afford the title compound **48** (429 mg, 0.99 mmol) in 55% yield. ^{1}H NMR (400 MHz, DMSO-d_6) δ 8.75 (s, 1H), 8.65 (t, J = 5.1 Hz, 1H), 7.68 (s, 1H), 6.94 (t, J = 9.5 Hz, 1H), 6.70 (dd, J = 8.7, 3.9 Hz, 1H), 4.68 (d, J = 5.0 Hz, 2H), 4.54 (t, J = 8.7 Hz, 2H), 4.29 (q, J = 7.1 Hz, 2H), 3.27 (t, J = 8.8 Hz, 2H), 1.32 (t, J = 7.1 Hz, 3H). ^{13}C NMR (100 MHz, DMSO-d_6) δ 162.56, 156.19, 155.66 (d, J_{C-F} = 236 Hz), 143.31, 141.90, 131.01, 129.62, 127.15, 123.65, 121.86 (d, J_{C-F} = 19 Hz), 114.33 (d, J_{C-F} = 24 Hz), 108.78 (d, J_{C-F} = 8 Hz), 93.85, 72.01, 60.62, 37.79, 29.00, 14.69. LC-MS: $[M + H]+$ = 434.03

*2-Bromo-4-(2,2-diethoxyethoxy)-1-fluorobenzene (**50**).* K_2CO_3 (109 g, 0.78 mol, 3 equiv) was added in one portion to a solution of 3-bromo-4-fluorophenol (**49**, 50 g, 0.26 mol, 1 equiv) and 2-bromo-1,1-diethoxyethane (67 g, 0.34 mol, 1.3 equiv) in DMF (250 mL). The suspension was heated to 110 °C and stirred overnight under N_2. After cooling to rt, the reaction was diluted with H_2O and extracted with EtOAc (2 × 500 mL). The combined organic phase was washed with brine and dried over anhydrous Na_2SO_4. The residue was purified on silica gel (0−10% EtOAc/hexane) to give the title compound (**50**) as a yellow oil (60.12 g, 196 mmol, 75% yield). ^{1}H NMR (400 MHz, CD_3OD) δ 7.13 (dd, J = 5.6, 2.8 Hz, 1H), 7.06−6.98 (m, 1H), 6.84 (td, J = 9.2, 3.2 Hz, 1H), 4.82 (t, J = 5.2 Hz, 1H), 3.97 (d, J = 5.2 Hz, 2H), 3.81-3.72 (m, 2H), 3.69-3.60 (m, 2H), 1.27 (t, J = 7.2 Hz, 6H). LC-MS: $[M + H]^+$ = 307.02

*4-Bromo-5-fluorobenzofuran (**51**) and 6-Bromo-5-fluorobenzofuran (**52**).* Compound **50** (100 g, 0.35 mmol) was added over 30 min at 100 °C to a solution of PPA (132.4 g, 0.39 mol) and toluene (300 mL). The reaction mixture was heated at 100 °C for 4 h. After cooling to rt, 400 mL of ice/H_2O was added and the mixture was extracted twice with hexane. The combined organic phase was washed with brine and dried over anhydrous Na_2SO_4. The residue was purified on silica gel (0−10% EtOAc/hexane) to give the title compound (**51**, **52**) as a mixture of isomers in 55% overall yield. LC-MS: $[M + H]^+$ = 214.94

*5-Fluorobenzofuran-4-carbonitrile (**53**) and 5-Fluorobenzofuran-6-carbonitrile (**54**).* $Pd(PPh_3)_4$ (16.2 g, 14 mmol) was added to a solution of **51** and **52** (31 g, 0.144 mol) and $Zn(CN)_2$ (25.3 g, 0.216 mol) in 100 mL of DMF. The reaction mixture was degassed with N_2 and stirred under an N_2 atmosphere for 24 h at 110 °C. After cooling to rt, H_2O was added and the mixture was extracted with EtOAc (2 × 100 mL). The combined organic phase was washed with brine and dried over anhydrous Na_2SO_4. The residue was purified on silica gel (0−20% EtOAc/hexane) to separate the desired isomer (**53**) in 40% yield as a white solid. ^{1}H NMR (400 MHz, CD_3OD) δ 8.10 (d, J = 2.0 Hz, 1H), 7.89-7.85 (m, 1H), 7.32-7.28 (m, 1H), 7.07 (d, J = 2.0 Hz, 1H). LC-MS: $[M + H]^+$ = 162.02

*(5-Fluorobenzofuran-4-yl)methanamine (**55**).* The desired isomer **53** (2.3 g, 14.55 mmol) in 10 mL of THF was treated with a 1 M solution of LAH in THF (36 mL) at 0 °C. Then, the temperature was increased to 50 °C and the reaction mixture was stirred overnight. After cooling to rt, the reaction was slowly quenched with satd. Na_2SO_4 at 0 °C and was then filtered and washed several times with EtOAc. Purification by flash chromatography (0−10% MeOH/DCM containing 1% Et_3N) gave the desired compound **55** (1.63 g, 10.1 mmol) in 70% yield. LC-MS: $[M + H]^+$ = 166.02

*(5-Fluoro-2,3-dihydrobenzofuran-4-yl)methanamine (**56**).* Pd/C (100 mg, 10% wt) was added to a solution of compound **55** (1 g, 6.02 mmol) in MeOH (50 mL). The reaction mixture was degassed with H_2 and stirred under a H_2 atmosphere for 6 h at 40 °C. The mixture was then filtered through celite and washed with MeOH. Concentration under reduced pressure followed by purification by flash chromatography (0−10% MeOH/DCM containing 1% Et_3N) gave the desired compound **56** (859 mg, 5.11 mmol) in 85% yield. ^{1}H NMR (400 MHz, DMSO-d_6) δ 8.21 (brs, 2H), 7.01 (dd, J = 10.1, 8.7 Hz, 1H), 6.80 (dd, J = 8.7, 4.0 Hz, 1H), 4.59 (t, J = 8.8 Hz, 2H), 3.97 (d, J = 1.3 Hz, 2H), 3.35 (d, J = 9.0 Hz, 2H). ^{13}C NMR (100 MHz, DMSO-d_6) δ 155.66 (d, J_{C-F} = 236 Hz), 156.21, 130.58, 118.43 (d, J_{C-F} = 19 Hz), 114.57 (d, J_{C-F} = 24 Hz), 110.31, 72.14, 28.66, 28.65. LC-MS: $[M + H]^+$ = 168.07

General Procedure for Seven-, Eight-, or Nine-Membered Lactam Rings: Scheme 3. *Protocol for the Coupling Reaction.* Palladium(II) acetate (0.1 equiv) and CataCXium A (0.2 equiv) were mixed together in DME (C = 0.2 M, degassed), and the resulting solution was added by a pipette to a stirred solution of **48** (1.0 equiv), the required amine (2.0 equiv), bis(pinacolato)diboron (2.0 equiv), and K_2CO_3 (3.0 equiv) in DME/H_2O (9:1, C = 0.2, degassed) at 80 °C. The reaction mixture was stirred at reflux overnight. Subsequently, the reaction mixture was concentrated and extracted with EtOAc, washed with water and brine, and then dried over Na_2SO_4. The mixture was concentrated, and the residue was purified by HPLC to afford the desired title compound in ∼50−60% yield.

Protocol for Boc Deprotection and Cyclization. The Boc-protected amine was treated with 25% TFA/DCM at rt for 1 h, after that the volatiles were removed in vacuum. The crude was diluted with EtOAc and washed with satd. aq. Na_2CO_3 and then brine. The organic layer was over Na_2SO_4 and concentrated *in vacuo* to provide the desired title compound, which was used as crude for the next step.

The crude compound (1 equiv) and LiOH (10 equiv) in THF/water (4:1, C = 0.2) were heated at 70 °C overnight. 3 N aq. HCl was added dropwise at 0 °C to pH 2−3. The mixture was concentrated, and the residue was purified by HPLC to afford the desired title compound as a white solid in 90% yield.

General Procedure for Substituted Eight-Membered-Ring Lactams Containing Both Hydrophobic and Hydrophilic Tail as R_1 Substituent: Scheme 4. An aliquot of 5-bromo-2-(trifluoromethyl)pyridin-4-yl methanol (**60**) was dissolved in dry DCM (C = 0.2 M), then to this solution, 1.5 equiv of Dess−Martin periodinane was added and the reaction mixture was stirred for 1 h, monitored by TLC. Upon completion and quenched with satd. NH_4Cl solution, it was then extracted with DCM and washed with water and brine. The organic layers were collected and combined, washed with brine, dried over anhydrous Na_2SO_4, and concentrated *in vacuo*. Purification was performed on silica gel normal phase column chromatography with increasing amounts of EtOAc in hexane to afford the desired aldehyde (**61**) in 90% yield.

MeOH (C = 0.2 M) was added to the obtained aldehyde, followed by 2.0 equiv of required amine and it was stirred for 2 h. After that, 2 equiv of $Na(CN)BH_3$ and 2 equiv of AcOH were added under an ice

https://doi.org/10.1021/acs.jmedchem.1c01059
J. Med. Chem. 2021, 64, 14540−14556

bath. Then, the ice bath was removed and the reaction mixture was stirred for 3 h and monitored by TLC. Upon completion, the mixture was concentrated, and the residue was purified by HPLC to afford the title compound **62** in ∼70% yield.

$(Boc)_2O$ (1.5 equiv), dissolved in dry DCM (C = 0.2 M), was added to the obtained secondary amine, and this was followed by 3 equiv of TEA, stirring for 1 h, and monitoring by TLC. Upon completion, the reaction was quenched with satd. NH_4Cl solution, then extracted with DCM and washed with brine. The organic layers were collected and combined, dried over anhydrous Na_2SO_4, and concentrated *in vacuo*. Purification was performed on silica gel normal phase column chromatography with increasing amounts of EtOAc in hexane to afford the Boc-protected secondary amine (**63**) in ∼90% yield.

Palladium (II) acetate (0.1 equiv) and CataCXium A (0.2 equiv) were mixed together in DME (C = 0.2 M, degassed) and resulting solution was added via a pipette to a stirred solution of compound **48**, compound **63** (2.0 equiv), bis(pinacolato)diboron (2.0 equiv) and K_2CO_3 (3.0 equiv) in DME/H_2O (9:1, C = 0.2 M, degassed) at 80 °C. The reaction mixture was stirred at reflux overnight. After that, the reaction mixture was concentrated and extracted with EtOAc, washed with water and brine, and then dried over Na_2SO_4. The mixture was concentrated, and residue was purified by HPLC to afford the title compound **64** as a white solid in 60% yield.

Compound **64** was treated with 25% TFA/DCM at 0 °C for 1 h, then the volatiles were removed in vacuum, and the residue was used as crude (**63**) for the next step.

A mixture of compound **65** (1 equiv) and LiOH (10 equiv) in THF (10 mL/mmol) and water (5 mL/mmol) was heated at 70 °C overnight. The mixture was concentrated, and the residue was then purified by preparative HPLC to afford **66** in 90% yield.

DIPEA (5 equiv) was added to a mixture of compound **66** (1 equiv) and HATU (1.1 equiv) in DMF (5 mL/mmol). The reaction mixture was stirred overnight. Then, it was concentrated, and the residue was purified by preparative HPLC to afford **28** in ∼90% yield.

*5-(((5-Fluoro-2,3-dihydrobenzofuran-4-yl)methyl)amino)-N-methyl-8-phenylimidazo[1,5-c]pyrimidine-1-carboxamide (**10**).* ^{1}H NMR (400 MHz, CD_3OD) δ 8.64 (s, 1H), 7.50−7.29 (m, 6H), 6.92−6.81 (m, 1H), 6.67 (dd, J = 8.7, 3.9 Hz, 1H), 4.83 (d, J = 1.2 Hz, 2H), 4.59 (t, J = 8.7 Hz, 2H), 3.38 (t, J = 8.7 Hz, 2H), 2.51 (s, 3H). LC-MS: $[M + H]^+$ = 418.16

*3-(((5-Fluoro-2,3-dihydrobenzofuran-4-yl)methyl)amino)-2,3a,5,7-tetraazadibenzo[cd,f]azulen-6(7H)-one (**11**).* ^{1}H NMR (400 MHz, DMSO-d_6) δ 9.50 (s, 1H), 8.67 (s, 1H), 8.53 (t, J = 5.1 Hz, 1H), 7.99 (s, 1H), 7.88−7.80 (m, 1H), 7.19 (dd, J = 6.1, 1.6 Hz, 2H), 7.02 (ddd, J = 8.3, 6.1, 2.4 Hz, 1H), 6.96 (dd, J = 10.3, 8.7 Hz, 1H), 6.71 (dd, J = 8.6, 3.9 Hz, 1H), 4.73 (d, J = 4.8 Hz, 2H), 4.56 (t, J = 8.7 Hz, 2H), 3.31 (d, J = 8.5 Hz, 2H). LC-MS: $[M + H]^+$ = 402.12

*12-(((5-Fluoro-2,3-dihydrobenzofuran-4-yl)methyl)amino)-4,5-dihydro-3H-2,4,11,12a-tetraazabenzo[4,5]cycloocta[1,2,3-cd]-inden-3-one (**12**).* ^{1}H NMR (400 MHz, DMSO-d_6) δ 8.79 (s, 1H), 8.53 (t, J = 5.1 Hz, 1H), 8.24 (t, J = 7.4 Hz, 1H), 7.53−7.35 (m, 4H), 7.33−7.24 (m, 1H), 7.03−6.90 (m, 1H), 6.72 (dd, J = 8.7, 3.9 Hz, 1H), 4.83−4.70 (m, 3H), 4.57 (t, J = 8.8 Hz, 2H), 4.03 (dd, J = 14.2, 5.7 Hz, 1H), 3.35 (t, J = 8.7 Hz, 2H). LC-MS: $[M + H]^+$ = 416.14

*13-(((5-Fluoro-2,3-dihydrobenzofuran-4-yl)methyl)amino)-5,6-dihydro-2,4,12,13a-tetraazabenzo[4,5]cyclonona[1,2,3-cd]inden-3(4H)-one (**13**).* ^{1}H NMR (400 MHz, DMSO-d_6) δ 8.74 (s, 1H), 8.44 (t, J = 5.1 Hz, 1H), 7.48 (t, J = 6.7 Hz, 1H), 7.38 (td, J = 7.4, 1.6 Hz, 1H), 7.29 (td, J = 7.4, 1.4 Hz, 1H), 7.22 (td, J = 7.5, 1.4 Hz, 2H), 7.10 (s, 1H), 6.96 (dd, J = 10.2, 8.6 Hz, 1H), 6.72 (dd, J = 8.6, 3.9 Hz, 1H), 4.80−4.64 (m, 2H), 4.56 (t, J = 8.8 Hz, 2H), 3.41−3.19 (m, 4H), 2.82 (dd, J = 9.0, 6.2 Hz, 2H). LC-MS: $[M + H]^+$ = 430.16

*12-(((5-Fluoro-2,3-dihydrobenzofuran-4-yl)methyl)amino)-4,5-dihydro-3H-2,4,6,11,12a-pentaazabenzo[4,5]cycloocta[1,2,3-cd]-inden-3-one (**14**).* ^{1}H NMR (400 MHz, DMSO-d_6) δ 8.82 (s, 1H), 8.65 (t, J = 5.1 Hz, 1H), 8.54 (dd, J = 4.8, 1.6 Hz, 1H), 8.47 (s, 1H), 7.92 (dd, J = 7.8, 1.6 Hz, 1H), 7.53−7.48 (m, 2H), 6.96 (dd, J = 10.3, 8.7 Hz, 1H), 6.72 (dd, J = 8.7, 3.9 Hz, 1H), 4.98-4.94 (m, 1H), 4.75 (s, 2H), 4.57-4.53 (m, 2H), 4.03 (m, 1H), 3.35 (t, J = 8.7 Hz, 2H). LC-MS: $[M + H]^+$ = 416.14

*6-Fluoro-12-(((5-fluoro-2,3-dihydrobenzofuran-4-yl)methyl)-amino)-4,5-dihydro-3H-2,4,11,12a-tetraazabenzo[4,5]cycloocta-[1,2,3-cd]inden-3-one (**15**).* ^{1}H NMR (400 MHz, DMSO-d_6) δ 8.84 (s, 1H), 8.64 (s, 1H), 8.49 (t, J = 7.2 Hz, 1H), 7.49 (s, 1H), 7.46−7.38 (m, 1H), 7.35−7.18 (m, 2H), 6.95 (t, J = 9.4 Hz, 1H), 6.71 (dd, J = 8.7, 3.8 Hz, 1H), 4.74 (s, 2H), 4.58 (dt, J = 17.7, 7.8 Hz, 3H), 4.31 (dd, J = 15.1, 5.8 Hz, 1H), 3.34 (t, J = 8.8 Hz, 2H). LC-MS: $[M + H]^+$ = 434.14

*7-Fluoro-12-(((5-fluoro-2,3-dihydrobenzofuran-4-yl)methyl)-amino)-4,5-dihydro-3H-2,4,11,12a-tetraazabenzo[4,5]cycloocta-[1,2,3-cd]inden-3-one (**16**).* ^{1}H NMR (400 MHz, DMSO-d_6) δ 8.79 (s, 1H), 8.57 (t, J = 5.1 Hz, 1H), 8.22 (d, J = 7.6 Hz, 1H), 7.50 (dd, J = 8.6, 5.7 Hz, 1H), 7.41 (s, 1H), 7.24 (td, J = 8.6, 2.7 Hz, 1H), 7.11 (dd, J = 9.2, 2.8 Hz, 1H), 6.96 (dd, J = 10.3, 8.7 Hz, 1H), 6.71 (dd, J = 8.7, 3.8 Hz, 1H), 4.77-4.33 (m, 3H), 4.56 (t, J = 8.7 Hz, 2H), 3.97 (dd, J = 14.6, 5.4 Hz, 1H), 3.35 (t, J = 8.7 Hz, 2H). LC-MS: $[M + H]^+$ = 434.14

*8-Fluoro-12-(((5-fluoro-2,3-dihydrobenzofuran-4-yl)methyl)-amino)-4,5-dihydro-3H-2,4,11,12a-tetraazabenzo[4,5]cycloocta-[1,2,3-cd]inden-3-one (**17**).* ^{1}H NMR (400 MHz, DMSO-d_6) δ 8.79 (s, 1H), 8.59 (t, J = 5.1 Hz, 1H), 8.21 (dd, J = 8.9, 5.6 Hz, 1H), 7.49 (s, 1H), 7.35−7.27 (m, 2H), 7.26−7.18 (m, 1H), 6.96 (dd, J = 10.3, 8.6 Hz, 1H), 6.71 (dd, J = 8.7, 3.9 Hz, 1H), 4.75 (q, J = 5.0 Hz, 3H), 4.56 (t, J = 8.8 Hz, 2H), 3.97 (dd, J = 14.7, 5.5 Hz, 1H), 3.35 (t, J = 8.7 Hz, 2H). LC-MS: $[M + H]^+$ = 434.14

*12-(((5-Fluoro-2,3-dihydrobenzofuran-4-yl)methyl)amino)-7-(trifluoromethyl)-4,5-dihydro-3H-2,4,11,12a-tetraazabenzo[4,5]-cycloocta[1,2,3-cd]inden-3-one (**18**).* ^{1}H NMR (400 MHz, DMSO-d_6) δ 8.82 (s, 1H), 8.69 (t, J = 5.1 Hz, 1H), 8.24 (dd, J = 8.8, 5.7 Hz, 1H), 7.74 (d, J = 8.3 Hz, 2H), 7.71−7.59 (m, 1H), 7.52 (s, 1H), 6.96 (t, J = 9.5 Hz, 1H), 6.72 (dd, J = 8.6, 3.8 Hz, 1H), 4.86 (dd, J = 14.6, 8.8 Hz, 1H), 4.76 (d, J = 4.5 Hz, 2H), 4.56 (t, J = 8.7 Hz, 2H), 4.11 (dd, J = 14.7, 5.5 Hz, 1H), 3.35 (t, J = 8.8 Hz, 2H). LC-MS: $[M + H]^+$ = 484.13

*12-(((5-Fluoro-2,3-dihydrobenzofuran-4-yl)methyl)amino)-8-(trifluoromethyl)-4,5-dihydro-3H-2,4,11,12a-tetraazabenzo[4,5]-cycloocta[1,2,3-cd]inden-3-one (**19**).* ^{1}H NMR (400 MHz, DMSO-d_6) δ 8.81 (s, 1H), 8.65 (t, J = 5.1 Hz, 1H), 8.28 (t, J = 7.0 Hz, 1H), 7.76 (dq, J = 3.7, 1.9 Hz, 2H), 7.60−7.43 (m, 2H), 6.96 (dd, J = 10.3, 8.7 Hz, 1H), 6.71 (dd, J = 8.6, 3.9 Hz, 1H), 4.85 (dd, J = 14.5, 8.8 Hz, 1H), 4.75 (d, J = 4.8 Hz, 2H), 4.57 (t, J = 8.8 Hz, 2H), 4.07 (dd, J = 14.6, 5.5 Hz, 1H), 3.36 (dd, J = 9.6, 7.5 Hz, 2H). LC-MS: $[M + H]^+$ = 484.13

*12-(((5-Fluoro-2,3-dihydrobenzofuran-4-yl)methyl)amino)-7-methyl-4,5-dihydro-3H-2,4,6,11,12a-pentaazabenzo[4,5]cycloocta-[1,2,3-cd]inden-3-one (**20**).* ^{1}H NMR (400 MHz, DMSO-d_6) δ 8.84 (s, 1H), 8.64 (d, J = 5.8 Hz, 1H), 8.40 (dd, J = 8.4, 6.0 Hz, 1H), 7.93 (d, J = 8.0 Hz, 1H), 7.49−7.39 (m, 2H), 6.96 (dd, J = 10.3, 8.7 Hz, 1H), 6.71 (dd, J = 8.6, 3.9 Hz, 1H), 4.95 (dd, J = 14.4, 8.5 Hz, 1H), 4.75 (d, J = 4.3 Hz, 2H), 4.56 (t, J = 8.8 Hz, 2H), 4.05 (dd, J = 14.4, 5.9 Hz, 1H), 3.34 (t, J = 8.7 Hz, 2H), 2.56 (s, 3H). LC-MS: $[M + H]^+$ = 431.15

*12-(((5-Fluoro-2,3-dihydrobenzofuran-4-yl)methyl)amino)-7-(trifluoromethyl)-4,5-dihydro-3H-2,4,6,11,12a-pentaazabenzo[4,5]-cycloocta[1,2,3-cd]inden-3-one (**21**).* ^{1}H NMR (400 MHz, DMSO-d_6) δ 8.84 (s, 1H), 8.77 (t, J = 5.1 Hz, 1H), 8.57−8.45 (m, 1H), 8.18 (d, J = 8.1 Hz, 1H), 7.94 (d, J = 8.1 Hz, 1H), 7.55 (s, 1H), 6.96 (dd, J = 10.3, 8.7 Hz, 1H), 6.72 (dd, J = 8.6, 3.9 Hz, 1H), 5.07 (dd, J = 14.4, 8.3 Hz, 1H), 4.77 (d, J = 4.8 Hz, 2H), 4.57 (t, J = 8.8 Hz, 2H), 4.10 (dd, J = 14.4, 6.0 Hz, 1H), 3.35 (t, J = 8.7 Hz, 2H). LC-MS: $[M + H]^+$ = 485.12

*12-(((5-Fluoro-2,3-dihydrobenzofuran-4-yl)methyl)amino)-7-(trifluoromethyl)-4,5-dihydro-3H-2,4,8,11,12a-pentaazabenzo[4,5]-cycloocta[1,2,3-cd]inden-3-one (**22**).* ^{1}H NMR (400 MHz, DMSO-d_6) δ 8.83 (s, 2H), 8.76 (t, J = 5.2 Hz, 1H), 8.23 (dd, J = 8.8, 5.7 Hz, 1H), 7.77 (s, 1H), 7.65 (s, 1H), 6.96 (t, J = 9.5 Hz, 1H), 6.72 (dd, J = 8.7, 3.8 Hz, 1H), 4.93 (dd, J = 14.5, 8.8 Hz, 1H), 4.77 (d, J = 4.8 Hz, 2H), 4.57 (t, J = 8.7 Hz, 2H), 4.17 (dd, J = 14.6, 5.6 Hz, 1H), 3.35 (t, J = 8.7 Hz, 2H). ^{13}C NMR (100 MHz, DMSO-d_6) δ 165.51, 156.94,

https://doi.org/10.1021/acs.jmedchem.1c01059
J. Med. Chem. 2021, 64, 14540−14556

156.23, 154.58, 150.73, 149.03, 143.77, 140.63, 134.49, 130.48, 129.69, 127.32, 124.27, 122.13, 121.29, 114.51, 114.27, 109.46, 108.86, 72.04, 43.46, 37.83, 29.07. LC-MS: $[M + H]^+$ = 485.13

11-(((5-Fluoro-2,3-dihydrobenzofuran-4-yl)methyl)amino)-6-methyl-5,6-dihydro-2,4,6,7,10,11a-hexaazacyclopenta[4,5]-cycloocta[1,2,3-cd]inden-3(4H)-one (**23**). ^{1}H NMR (400 MHz, DMSO-d_6) δ 8.74 (s, 1H), 8.45 (t, J = 7.2 Hz, 1H), 8.37 (t, J = 5.2 Hz, 1H), 7.64 (s, 1H), 7.44 (s, 1H), 6.93 (dd, J = 10.4, 8.7 Hz, 1H), 6.69 (dd, J = 8.6, 3.9 Hz, 1H), 4.78−4.60 (m, 3H), 4.54 (t, J = 8.7 Hz, 2H), 4.18 (dd, J = 16.0, 5.7 Hz, 1H), 3.88 (s, 3H), 3.30 (t, J = 8.7 Hz, 2H). LC-MS: $[M + H]^+$ = 420.15

11-(((5-Fluoro-2,3-dihydrobenzofuran-4-yl)methyl)amino)-4,5-dihydro-3H-6-thia-2,4,10,11a-tetraazacyclopenta[4,5]cycloocta-[1,2,3-cd]inden-3-one (**24**). ^{1}H NMR (400 MHz, DMSO-d_6) δ 8.78 (s, 1H), 8.49 (s, 1H), 8.39 (t, J = 7.1 Hz, 1H), 7.55 (s, 1H), 7.50 (d, J = 5.2 Hz, 1H), 7.27 (d, J = 5.3 Hz, 1H), 6.99−6.88 (m, 1H), 6.70 (dd, J = 8.7, 3.9 Hz, 1H), 4.86 (dd, J = 15.7, 8.4 Hz, 1H), 4.73 (d, J = 4.8 Hz, 2H), 4.55 (t, J = 8.7 Hz, 2H), 4.02 (dd, J = 15.9, 5.8 Hz, 1H), 3.31 (d, J = 8.7 Hz, 2H). LC-MS: $[M + H]^+$ = 422.10

11-(((5-Fluoro-2,3-dihydrobenzofuran-4-yl)methyl)amino)-4,5-dihydro-3H-8-thia-2,4,10,11a-tetraazacyclopenta[4,5]cycloocta-[1,2,3-cd]inden-3-one (**25**). ^{1}H NMR (400 MHz, DMSO-d_6) d 8.80 (s, 1H), 8.57 (s, 1H), 8.31 (t, J = 7.2 Hz, 1H), 7.57−7.35 (m, 2H), 7.01 (d, J = 5.1 Hz, 1H), 6.94 (dd, J = 10.3, 8.6 Hz, 1H), 6.70 (dd, J = 8.7, 3.9 Hz, 1H), 4.72 (d, J = 4.3 Hz, 2H), 4.67−4.49 (m, 3H), 3.99 (dd, J = 15.0, 5.7 Hz, 1H), 3.31 (d, J = 8.7 Hz, 2H). LC-MS: $[M + H]^+$ = 422.10

12-(((5-Fluoro-2,3-dihydrobenzofuran-4-yl)methyl)amino)-4-methyl-7-(trifluoromethyl)-4,5-dihydro-3H-2,4,8,11,12a-pentaazabenzo[4,5]cycloocta[1,2,3-cd]inden-3-one (**26**). ^{1}H NMR (400 MHz, CD_3OD) δ 8.84 (s, 1H), 8.74 (s, 1H), 7.96 (s, 1H), 7.69 (s, 1H), 6.87 (t, J = 9.5 Hz, 1H), 6.66 (dd, J = 8.8, 3.7 Hz, 1H), 5.54 (d, J = 14.8 Hz, 1H), 4.81 (d, J = 6.1 Hz, 2H), 4.61 (t, J = 8.8 Hz, 2H), 4.28 (d, J = 14.8 Hz, 1H), 3.43 (t, J = 8.8 Hz, 2H), 3.16 (s, 3H). LC-MS: $[M + H]^+$ = 499.14

4-Ethyl-12-(((5-fluoro-2,3-dihydrobenzofuran-4-yl)methyl)-amino)-7-(trifluoromethyl)-4,5-dihydro-3H-2,4,8,11,12a-pentaazabenzo[4,5]cycloocta[1,2,3-cd]inden-3-one (**27**). ^{1}H NMR (400 MHz, DMSO-d_6) δ 8.86 (s, 1H), 8.85−8.74 (m, 2H), 8.15 (s, 1H), 7.63 (s, 1H), 6.96 (dd, J = 10.3, 8.7 Hz, 1H), 6.72 (dd, J = 8.7, 3.9 Hz, 1H), 5.25 (d, J = 14.8 Hz, 1H), 4.77 (d, J = 4.8 Hz, 2H), 4.56 (t, J = 8.8 Hz, 2H), 4.32 (d, J = 14.8 Hz, 1H), 3.78 (dq, J = 13.8, 6.9 Hz, 1H), 3.34 (t, J = 8.9 Hz, 2H), 3.12 (dq, J = 13.6, 6.7 Hz, 1H), 1.10 (t, J = 7.0 Hz, 3H). LC-MS: $[M + H]^+$ = 513.15

12-(((5-Fluoro-2,3-dihydrobenzofuran-4-yl)methyl)amino)-4-isopropyl-7-(trifluoromethyl)-4,5-dihydro-3H-2,4,8,11,12a-pentaazabenzo[4,5]cycloocta[1,2,3-cd]inden-3-one (**28**). ^{1}H NMR (400 MHz, DMSO-d_6) δ 9.02−8.67 (m, 2H), 8.11 (d, J = 7.3 Hz, 1H), 7.62 (d, J = 7.4 Hz, 1H), 6.96 (q, J = 9.1 Hz, 1H), 6.72 (dq, J = 8.4, 3.7 Hz, 1H), 5.26 (dd, J = 15.2, 7.2 Hz, 2H), 4.78 (d, J = 6.4 Hz, 2H), 4.56 (q, J = 8.5 Hz, 2H), 4.39 (dd, J = 15.4, 7.0 Hz, 1H), 4.27 (q, J = 7.3 Hz, 1H), 3.35 (q, J = 8.5 Hz, 2H), 1.41−1.23 (m, 3H), 1.23−1.06 (m, 3H). ^{13}C NMR (100 MHz, DMSO-d_6) δ 163.79, 156.22, 155.66 (d, J_{C-F} = 236 Hz), 150.39, 147.42, 145.53 (d, J_{C-F} = 33 Hz), 143.67, 141.16, 135.20, 129.88, 129.61 (d, J_{C-F} = 5 Hz), 126.93, 125.70, 122.17 (q, J_{C-F} = 272 Hz), 122.11, 121.94, 121.38, 114.37 (d, J_{C-F} = 24 Hz), 109.3, 108.78 (d, J_{C-F} = 8 Hz), 72.0, 50.7, 48.4, 29.0, 20.8, 19.6. LC-MS: $[M + H]^+$ = 526.95

4-Cyclopropyl-12-(((5-fluoro-2,3-dihydrobenzofuran-4-yl)-methyl)amino)-7-(trifluoromethyl)-4,5-dihydro-3H-2,4,8,11,12a-pentaazabenzo[4,5]cycloocta[1,2,3-cd]inden-3-one (**29**). ^{1}H NMR (400 MHz, CD_3OD) δ 8.84 (s, 1H), 8.74 (s, 1H), 7.86 (s, 1H), 7.70 (s, 1H), 6.86 (t, J = 9.6 Hz, 1H), 6.65 (dd, J = 8.7, 4.0 Hz, 1H), 5.42 (d, J = 14.7 Hz, 1H), 4.81 (d, J = 6.1 Hz, 2H), 4.59 (t, J = 8.9 Hz, 2H), 4.37 (d, J = 14.9 Hz, 1H), 3.42 (t, J = 8.7 Hz, 2H), 2.55 (s, 1H), 1.16 (s, 1H), 1.00 (d, J = 5.5 Hz, 2H), 0.94−0.77 (m, 1H). LC-MS: $[M + H]^+$ = 525.15

4-Cyclobutyl-12-(((5-fluoro-2,3-dihydrobenzofuran-4-yl)methyl)-amino)-7-(trifluoromethyl)-4,5-dihydro-3H-2,4,8,11,12a-pentaazabenzo[4,5]cycloocta[1,2,3-cd]inden-3-one (**30**). ^{1}H NMR (400 MHz, DMSO-d_6) δ 8.86 (s, 1H), 8.83−8.71 (m, 2H), 7.86 (s, 1H), 7.62 (s, 1H), 6.96 (dd, J = 10.3, 8.6 Hz, 1H), 6.71 (dd, J = 8.6, 3.9 Hz, 1H), 5.22 (d, J = 15.0 Hz, 1H), 4.77 (d, J = 4.9 Hz, 2H), 4.56 (t, J = 8.8 Hz, 2H), 4.40 (d, J = 15.1 Hz, 1H), 4.34−4.19 (m, 1H), 3.36−3.32 (m, 2H), 2.63−2.54 (m, 1H), 2.40−2.07 (m, 3H), 1.70 (ddt, J = 25.8, 10.6, 7.5 Hz, 2H). LC-MS: $[M + H]^+$ = 539.17

4-(2,2-Difluoroethyl)-12-(((5-fluoro-2,3-dihydrobenzofuran-4-yl)-methyl)amino)-7-(trifluoromethyl)-4,5-dihydro-3H-2,4,8,11,12a-pentaazabenzo[4,5]cycloocta[1,2,3-cd]inden-3-one (**31**). ^{1}H NMR (400 MHz, DMSO-d_6) δ 8.86-8.80 (m, 2H), 8.27 (s, 1H), 7.66 (s, 1H), 6.96 (t, J = 8.8 Hz, 1H), 6.71 (dd, J = 8.6, 3.8 Hz, 1H), 6.24 (t, J = 56.4 Hz, 1H), 5.40 (d, J = 14.8 Hz, 1H), 4.76 (d, J = 4.0 Hz, 1H), 4.56 (d, J = 8.8 Hz, 1H), 4.37 (d, J = 14.8 Hz, 1H), 4.13-4.03 (m, 1H), 3.77-3.68 (m, 2H), 3.36−3.32 (m, 2H). LC-MS: $[M + H]^+$ = 548.86

4-(2,2-Difluoropropyl)-12-(((5-fluoro-2,3-dihydrobenzofuran-4-yl)methyl)amino)-7-(trifluoromethyl)-4,5-dihydro-3H-2,4,8,11,12a-pentaazabenzo[4,5]cycloocta[1,2,3-cd]inden-3-one (**32**). ^{1}H NMR (400 MHz, DMSO-d_6) δ 8.87 (d, J = 2.0 Hz, 2H), 8.83 (s, 1H), 8.18 (s, 1H), 7.67 (s, 1H), 6.96 (dd, J = 10.3, 8.7 Hz, 1H), 6.71 (dd, J = 8.7, 3.9 Hz, 1H), 5.48−5.28 (m, 1H), 4.77 (d, J = 4.2 Hz, 2H), 4.56 (t, J = 8.8 Hz, 2H), 4.41−4.20 (m, 2H), 3.62 (td, J = 14.3, 10.0 Hz, 1H), 3.34 (t, J = 8.7 Hz, 2H), 1.66 (t, J = 19.3 Hz, 3H). LC-MS: $[M + H]^+$ = 563.05

12-(((5-Fluoro-2,3-dihydrobenzofuran-4-yl)methyl)amino)-4-(2,2,2-trifluoroethyl)-7-(trifluoromethyl)-4,5-dihydro-3H-2,4,8,11,12a-pentaazabenzo[4,5]cycloocta[1,2,3-cd]inden-3-one (**33**). ^{1}H NMR (400 MHz, DMSO-d_6) δ 8.85 (dd, J = 14.5, 5.1 Hz, 3H), 8.36 (s, 1H), 7.69 (s, 1H), 7.02−6.92 (m, 1H), 6.72 (dd, J = 8.6, 3.9 Hz, 1H), 5.43 (d, J = 15.1 Hz, 1H), 4.77 (d, J = 5.0 Hz, 2H), 4.69−4.51 (m, 3H), 4.38 (d, J = 15.1 Hz, 1H), 4.21−4.11 (m, 1H), 3.34 (t, J = 8.8 Hz, 2H). LC-MS: $[M + H]^+$ = 567.13

4-(3,3-Difluorocyclobutyl)-12-(((5-fluoro-2,3-dihydrobenzofuran-4-yl)methyl)amino)-7-(trifluoromethyl)-4,5-dihydro-3H-2,4,8,11,12a-pentaazabenzo[4,5]cycloocta[1,2,3-cd]inden-3-one (**34**). ^{1}H NMR (400 MHz, DMSO-d_6) δ 8.87 (s, 1H), 8.81 (d, J = 7.0 Hz, 2H), 8.02 (s, 1H), 7.66 (s, 1H), 6.96 (t, J = 9.5 Hz, 1H), 6.72 (dd, J = 8.6, 3.8 Hz, 1H), 5.34 (d, J = 15.2 Hz, 1H), 4.77 (d, J = 4.8 Hz, 2H), 4.56 (t, J = 8.8 Hz, 2H), 4.36 (d, J = 15.1 Hz, 1H), 4.21 (td, J = 8.3, 3.7 Hz, 1H), 3.34 (t, J = 8.8 Hz, 2H), 3.19−3.02 (m, 2H), 2.92 (d, J = 19.6 Hz, 2H). LC-MS: $[M + H]^+$ = 575.15

12-(((5-Fluoro-2,3-dihydrobenzofuran-4-yl)methyl)amino)-4-(2-hydroxy-2-methylpropyl)-7-(trifluoromethyl)-4,5-dihydro-3H-2,4,8,11,12a-pentaazabenzo[4,5]cycloocta[1,2,3-cd]inden-3-one (**35**). ^{1}H NMR (400 MHz, CD_3OD) δ 8.83 (s, 1H), 8.75 (s, 1H), 8.05 (s, 1H), 7.69 (s, 1H), 6.93−6.81 (m, 1H), 6.66 (dd, J = 8.7, 3.9 Hz, 1H), 5.42 (d, J = 14.9 Hz, 1H), 4.84 (d, J = 1.0 Hz, 2H), 4.65−4.52 (m, 2H), 4.08 (d, J = 14.2 Hz, 1H), 3.42 (t, J = 8.7 Hz, 2H), 3.08 (d, J = 14.2 Hz, 1H), 2.68 (s, 1H), 1.42−1.18 (m, 6H). LC-MS: $[M + H]^+$ = 557.18

12-(((5-Fluoro-2,3-dihydrobenzofuran-4-yl)methyl)amino)-4-(tetrahydro-2H-pyran-4-yl)-7-(trifluoromethyl)-4,5-dihydro-3H-2,4,8,12a-tetraazabenzo[4,5]cycloocta[1,2,3-cd]inden-3-one (**36**). ^{1}H NMR (400 MHz, CD_3OD) δ 8.81 (s, 1H), 8.17 (d, J = 8.1 Hz, 1H), 7.88 (d, J = 8.2 Hz, 1H), 7.66 (s, 1H), 6.94−6.82 (m, 1H), 6.66 (dd, J = 8.7, 3.9 Hz, 1H), 5.56−5.45 (m, 1H), 4.88 (s, 2H), 4.65−4.50 (m, 2H), 4.45-4.41 (m, 1H), 4.12−3.93 (m, 2H), 3.55−3.39 (m, 4H), 3.39−3.36 (m, 2H), 2.58-2.50 (m, 1H), 2.30-2.25 (m, 1H), 1.65-1.60 (m, 1H), 1.38-1.34 (m, 1H). LC-MS: $[M + H]^+$ = 569.18

4-(2,6-Dimethyltetrahydro-2H-pyran-4-yl)-12-(((5-fluoro-2,3-dihydrobenzofuran-4-yl)methyl)amino)-7-(trifluoromethyl)-4,5-dihydro-3H-2,4,8,11,12a-pentaazabenzo[4,5]cycloocta[1,2,3-cd]inden-3-one (**37**). ^{1}H NMR (400 MHz, DMSO-d_6) δ 8.87 (d, J = 3.9 Hz, 1H), 8.82 (d, J = 2.9 Hz, 1H), 8.78 (s, 1H), 8.16 (d, J = 16.5 Hz, 1H), 7.62 (d, J = 4.4 Hz, 1H), 6.96 (dd, J = 10.3, 8.7 Hz, 1H), 6.71 (dd, J = 8.6, 3.9 Hz, 1H), 5.32 (dd, J = 27.2, 14.9 Hz, 1H), 4.76 (d, J = 4.5 Hz, 2H), 4.56 (t, J = 8.8 Hz, 2H), 4.41 (dd, J = 14.9, 5.2 Hz, 1H), 3.95 (dd, J = 7.3, 4.9 Hz, 1H), 3.47 (dtd, J = 10.9, 6.2, 1.9 Hz, 1H), 3.34 (t, J = 8.7 Hz, 2H), 2.41−2.24 (m, 1H), 1.86 (ddd, J = 47.0, 23.6, 11.9 Hz, 1H), 1.59 (dt, J = 12.9, 7.4 Hz, 1H), 1.17−0.99 (m, 6H), 0.83 (dt, J = 12.2, 5.7 Hz, 1H). LC-MS: $[M + H]^+$ = 597.21

12-(((5-Fluoro-2,3-dihydrobenzofuran-4-yl)methyl)amino)-4-((1-hydroxycyclopropyl)methyl)-7-(trifluoromethyl)-4,5-dihydro-3H-

https://doi.org/10.1021/acs.jmedchem.1c01059
J. Med. Chem. 2021, 64, 14540−14556

*2,4,8,11,12a-pentaazabenzo[4,5]cycloocta[1,2,3-cd]inden-3-one (**38**).* ^{1}H NMR (400 MHz, CD_3OD) δ 8.82 (s, 1H), 8.76 (s, 1H), 7.99 (s, 1H), 7.67 (s, 1H), 6.89−6.79 (m, 1H), 6.63 (dd, J = 8.7, 3.8 Hz, 1H), 5.46 (d, J = 15.0 Hz, 1H), 4.86 (s, 2H), 4.82 (d, J = 14.9 Hz, 1H), 4.58 (td, J = 8.7, 1.2 Hz, 2H), 3.95 (d, J = 14.4 Hz, 1H), 3.49 (d, J = 14.5 Hz, 1H), 3.41 (t, J = 8.7 Hz, 2H), 0.91 (t, J = 2.4 Hz, 1H), 0.86−0.72 (m, 3H). LC-MS: $[M + H]^+$ = 555.16

*12-(((5-Fluoro-2,3-dihydrobenzofuran-4-yl)methyl)amino)-4-((3-hydroxy-3-methylcyclobutyl)-methyl)-7-(trifluoromethyl)-4,5-dihydro-3H-2,4,8,11,12a-pentaazabenzo[4,5]cycloocta[1,2,3-cd]inden-3-one (**39**).* ^{1}H NMR (400 MHz, CD_3OD) δ 8.83 (s, 1H), 8.76 (q, J = 1.5 Hz, 1H), 7.94 (s, 1H), 7.66 (s, 1H), 6.86 (t, J = 9.7 Hz, 1H), 6.65 (d, J = 8.5 Hz, 1H), 5.41 (d, J = 14.9 Hz, 1H), 4.84 (d, J = 1.0 Hz, 2H), 4.59 (t, J = 8.8 Hz, 2H), 4.34 (d, J = 14.9 Hz, 1H), 4.00 (dd, J = 13.6, 7.3 Hz, 1H), 3.41 (t, J = 8.7 Hz, 2H), 3.26 (dd, J = 13.6, 6.8 Hz, 1H), 2.31 (q, J = 8.1 Hz, 1H), 2.14 (ddt, J = 17.7, 12.2, 5.1 Hz, 2H), 2.05−1.87 (m, 2H), 1.33 (s, 3H). LC-MS: $[M + H]^+$ = 583.20

*12-(((5-Fluoro-2,3-dihydrobenzofuran-4-yl)methyl)amino)-4-((tetrahydro-2H-pyran-4-yl)methyl)-7-(trifluoromethyl)-4,5-dihydro-3H-2,4,8,11,12a-pentaazabenzo[4,5]cycloocta[1,2,3-cd]inden-3-one (**40**).* ^{1}H NMR (400 MHz, CD_3OD) δ 8.83 (s, 1H), 8.77 (brs, 1H), 8.02 (s, 1H), 7.70 (s, 1H), 6.95−6.80 (m, 1H), 6.66 (dd, J = 8.7, 3.9 Hz, 1H), 5.45 (d, J = 14.8 Hz, 1H), 4.60 (t, J = 8.8 Hz, 2H), 4.39 (d, J = 15.0 Hz, 1H), 3.96 (s, 2H), 3.85 (s, 1H), 3.56−3.35 (m, 4H), 3.42 (m, 2H), 3.15 -3.10 (m, 1H), 2.32−2.22 (m, 1H), 1.57 (dd, J = 24.7, 12.9 Hz, 2H), 1.49−1.26 (m, 2H). LC-MS: $[M + H]^+$ = 583.20

*12-(((5-Fluoro-2,3-dihydrobenzofuran-4-yl)methyl)amino)-4-((1-methylpiperidin-4-yl)methyl)-7-(trifluoromethyl)-4,5-dihydro-3H-2,4,8,11,12a-pentaazabenzo[4,5]cycloocta[1,2,3-cd]inden-3-one (**41**).* ^{1}H NMR (400 MHz, CD_3OD) δ 8.85 (s, 1H), 8.75 (s, 1H), 8.00 (s, 1H), 7.69 (s, 1H), 6.87 (t, J = 9.5 Hz, 1H), 6.66 (d, J = 8.9 Hz, 1H), 5.46 (d, J = 14.9 Hz, 1H), 4.81 (d, J = 6.1 Hz, 2H), 4.61 (t, J = 8.7 Hz, 2H), 4.32 (d, J = 15.0 Hz, 1H), 3.92 (dd, J = 13.7, 8.9 Hz, 1H), 3.58 (t, J = 11.7 Hz, 2H), 3.43 (t, J = 8.7 Hz, 2H), 3.11 (dd, J = 13.7, 5.7 Hz, 1H), 2.99 (dd, J = 29.9, 11.6 Hz, 2H), 2.90 (s, 3H), 2.23 (s, 1H), 2.07 (d, J = 14.4 Hz, 1H), 1.98 (d, J = 14.6 Hz, 1H), 1.64 (d, J = 14.1 Hz, 2H). LC-MS: $[M + H]^+$ = 596.23

*4-((1,4-Dioxan-2-yl)methyl)-12-(((5-fluoro-2,3-dihydrobenzofuran-4-yl)methyl)amino)-7-(trifluoromethyl)-4,5-dihydro-3H-2,4,8,11,12a-pentaazabenzo[4,5]cycloocta[1,2,3-cd]inden-3-one (**42**).* ^{1}H NMR (400 MHz, CD_3OD) δ 8.82 (t, J = 4.7 Hz, 2H), 7.95 (d, J = 4.3 Hz, 1H), 7.69 (s, 1H), 6.86 (t, J = 9.5 Hz, 1H), 6.71−6.58 (m, 1H), 5.47 (dd, J = 15.0, 9.3 Hz, 1H), 4.81 (d, J = 6.1 Hz, 2H), 4.68−4.49 (m, 3H), 4.09−3.76 (m, 4H), 3.76−3.47 (m, 4H), 3.41 (q, J = 8.6 Hz, 3H). LC-MS: $[M + H]^+$ = 585.17

EED-H3K27Me3 Peptide Competition Binding Assay by AlphaScreen. To assess the potency of the compounds in the EED-$H_3K_{27}Me_3$ competitive binding assay, the compounds were serially diluted up to 3-fold in DMSO to obtain a total of 12 concentrations. Then, 2.5 μL of a solution of compounds at each concentration was transferred into 384-well PerkinElmer OptiPlate-384 white plates. Solutions (5 μL) containing 20 nM EED (1-441)-His protein in the buffer (25 mM HEPES, pH 8, 0.02% Tween-20, 0.5% BSA) were added to the wells and then incubated with the compound for 15 min. Solutions (2.5 μL) containing 20 nM biotin-H3K27Me_3 (19-33) peptide in the buffer (25 mM HEPES, pH 8, 0.02% Tween-20, 0.5% BSA) were added to the wells and incubated with the compound for 30 min. An AlphaScreen detection beads mix was prepared immediately before use by mixing nickel chelate acceptor beads and streptavidin donor beads in a 1:1 ratio (PerkinElmer, Product No. 6760619C/M/R) into the buffer described above. Then, 10 μL of detection beads mix was added to the plate which was incubated in the dark at rt for 1 h. The final concentration of donor and acceptor beads was 10 μg/mL in each case. Plates were read on a CLARIOStar plate reader (BMG Labtech) using the AlphaScreen setting adapted for optimal signal detection with a 615 nm filter, after sample excitation at 680 nm. The emission signal at 615 nm was used to quantify the inhibition of the compounds. AlphaScreen signals were normalized based on the reading coming from the positive (maximum signal control) and negative controls (minimum signal control) to give a percentage of activities remaining. The data were then fit to a dose−response equation to obtain the IC_{50} values.

Cell Growth Inhibition. The human B cell lymphoma cell KARPAS422 lines were purchased from the American Type Culture Collection (ATCC) and were cultured using standard cell culture conditions in RPMI-1640 (Invitrogen, Cat #11875) supplemented with 10% FBS (Invitrogen, Cat #10099-141) in a humidified incubator at 37 °C, 5% CO_2. To assess the effect of EED inhibitors on cell growth, cells were seeded in 96-well cell culture plates at a density of 2000−3000 cells/well in 200 μL of culture medium and treated with serially diluted compounds for 7 days at 37 °C in an atmosphere of 5% CO_2. Cell growth was evaluated by a lactate dehydrogenase-based WST-8 assay using a Tecan Infinite M1000 multimode microplate reader. The WST-8 reagent was added to the plate, incubated for 1−4 h, and read at 450 nm. The readings were normalized to the DMSO-treated cells, and the IC_{50} was calculated by nonlinear regression analysis using GraphPad Prism 7.00.

Pharmacodynamics and Efficacy Studies in Mice. Animal experiments were performed under an approved animal protocol (Protocol ID: PRO00007499, PI: Shaomeng Wang) by the Institutional Animal Care & Committee of the University of Michigan. Xenograft tumors were established by injecting 1×10^7 KARPAS422 human B cell lymphoma cells in 50% Matrigel subcutaneously on the dorsal side of severe combined immune-deficient (SCID) mice, obtained from Charles River, with one tumor per mouse. When tumors reached ∼100 mm^3, the mice were randomly assigned to treatment and vehicle control groups. The animals were monitored daily for signs of toxicity and weighed two to three times per week during the treatment period and at least weekly after the treatment ended. Tumor size was measured utilizing electronic calipers two to three times per week during the treatment period and at least weekly after the treatment ended. Tumor volume was calculated as $V = L \times W^2/2$, where L is the length and W is the width of the tumor. EED inhibitors were formulated as a suspension in PEG 200 and administered orally by gavage at indicated doses. When applicable, results are presented as mean ± SEM. Graphing and statistical analysis were performed using GraphPad Prism 7.00

Molecular Modeling. The co-crystal structure of EED/EEDi-1056 (PDB accession code: 6W7G)[22] was used to construct the binding modes of compounds **10** and **22** with EED. The missing side-chain atoms of EED were rebuilt using the MOE[31] program. Protonation states of the amino acids in EED at the pH 7.0 condition were assigned using the "protonate 3D" module in MOE. Structures of the compounds were depicted and optimized using MOE. We used the GOLD suite (CSD Discovery 2021)[32,33] to perform the docking calculation by setting the binding site centered at R367 in EED with a radius of 20 Å. Default parameters and the PLP fitness function were used. A total of 15 binding poses of each compound were saved, and the highest-ranked pose of each compound was selected as the binding model after the structural analysis.

Expression and Purification of EED Protein. The human EED (residues 77-441 with M370T mutation) was expressed and purified as previously described.[22] Briefly, transformed cells were induced with 0.4 mM IPTG and expressed at 20 °C overnight. Cell pellet was lysed in buffer containing 25 mM Tris pH 7.5, 200 mM NaCl, 0.1% β-mercaptoethanol, 10 μg/mL aprotinin, and 1 μg/mL leupeptin. The resulting supernatant was incubated with Ni-NTA resin at 4 °C for 1 h and then washed with buffer containing 25 mM Tris pH 7.5, 200 mM NaCl, and 10 mM imidazole. The protein was eluted from Ni-NTA resin with 25 mL of buffer composed of 25 mM Tris pH 7.5, 200 mM NaCl, and 300 mM imidazole, treated with TEV protease to remove the affinity tag and dialyzed against 1 L of buffer containing 25 mM Tris pH 7.5, 150 mM NaCl, and 0.1% mercaptoethanol overnight. EED was further purified by size exclusion chromatography on a HiLoad 16/60 Superdex 200 column (GE Healthcare) pre-equilibrated with 25 mM Tris pH 7.5, 200 mM NaCl, and 1 mM DTT. Purified protein was dialyzed into 20 mM Tris pH 8.7, 150 mM NaCl, and 1 mM TCEP and concentrated to 4 mg/mL for crystallization.

https://doi.org/10.1021/acs.jmedchem.1c01059
J. Med. Chem. 2021, 64, 14540−14556

Crystallization and Structure Determination of EED. Human EED was crystallized by sitting drop vapor diffusion at 20 °C. Drops producing crystals contained concentrated protein (4 mg/mL in 20 mM Tris pH 8.7, 150 mM NaCl, 1 mM TCEP) mixed with an equal volume of well solution containing 100 mM Tris pH 8.5, 4.3−4.5 M sodium formate, 20% glycerol, and 10 mM tris(2-carboxyethyl)-phosphine. Crystals were transferred into a soak solution consisting of well solution supplemented with 1 mM **18** or 5 mM **32** and incubated at 20 °C for 24 h and then flash-frozen in liquid nitrogen.

Diffraction data were collected on the Advanced Photon Source LS-CAT beamlines 21-ID-G or 21-ID-F (Table S1), processed with HKL2000,[34] and solved by molecular replacement in Molrep[35] using an in-house structure of EED as a search model. Iterative model building and refinement were performed using COOT[36] and BUSTER,[37] respectively. Ligand restraints were generated using GRADE.[37]

The structures of EED with inhibitors **18** (PDB ID: 7MSB) and **32** (PDB ID: 7MSD) were solved in $P2_12_12_1$ to 1.9 Å and 2.20 Å resolution, respectively, with one chain of protein per asymmetric unit. The overall structure of the protein was highly similar between **18** and **32**, with an RMSD of 0.2511 Å based on SSM superpositioning in COOT.[36] Ligand density was observed in the methyllysine binding site for each inhibitor (Figure S3). N-terminal residues 77−80 and C-terminal residues 440−441 were disordered in both structures.

Pharmacokinetic Studies in Mice. PK studies were performed with male CD1 mice, weighing 18−20 g. The first group of mice was dosed IV *via* a bolus in the tail vein with a dose level of 2 mg/kg, and the second group of mice was dosed orally as a single esophageal gavage with a dose level of 10 mg/kg. The formulation was freshly prepared before use. For the IV route, the compound was formulated in 10% DMSO, 5% Solutol HS15, and 85% saline as a clear solution. For the oral route, the compound was formulated in 20% DMSO, 10% Solutol HS15, and 70% distilled water as a homogeneous suspension. Blood samples were collected at the following time points: IV, 0.033, 0.083, 0.25, 0.5, 1, 2, 4, 6, 8, and 24 h after dosing (n = 3 mice per sampling time); PO, 0.25, 0.5, 1, 2, 4, 6, 8, and 24 h after dosing (n = 3 mice per sampling time). Each mouse was sampled once and then euthanized. Blood was kept on ice. Within 1 h after sampling, blood was centrifuged at 3900 rpm for 15 min, the plasma supernatant was mixed three times with acetonitrile and centrifuged. Then the supernatant was diluted one time with water. Diluted supernatant (5 μL) was injected into the LC/MS/MS system for quantitative analysis.

hERG Manual Patch Clamp Assay. The potential inhibitory effect of test article on human Ether-à-go-go related gene (hERG) channel was evaluated by a manual patch-clamp system according to the protocols as described in this report. HEK293 cell line stably transfected with hERG gene was employed in this study and Dofetilide was used as a positive control to ensure the good quality of the assay. HEK293 cell line stably expressing hERG channel (Cat# K1236) was purchased from Invitrogen. The cells were cultured in 85% DMEM, 10% dialyzed FBS, 0.1 mM NEAA, 25 mM HEPES, 100 U/mL penicillin-streptomycin, 5 μg/mL Blasticidin, and 400 μg/mL Geneticin. The cells were split using TrypLE Express about three times a week and maintained between ∼40% to ∼80% confluence. Before the assay, the cells were onto the coverslips at 5 × 105 cells/per 6 cm cell culture dish and induced with doxycycline at 1 μg/mL for 48 h. The external bathing solution contained 132 mM NaCl, 4 mM KCl, 1.8 mM $CaCl_2$, 0.5 $MgCl_2$, 11.1 mM glucose, and 10 HEPES (pH adjusted to 7.35 M with NaOH). The internal patch pipette solution contained 140 mM KCl, 2 mM $MgCl_2$, 10 mM EGTA, 10 mM HEPES, and 5 mM MgATP (pH adjusted to 7.35 with KOH). PatchMaster software was used to extract the peak current from the original data.

Liver Microsomal Stability (LMS) Assay. For the microsomal stability assay, two separate experiments were performed as follows: (a) With Cofactors (NADPH): 25 μL of 10 mM NADPH added to the incubations. The final concentrations of microsomes and NADPH were 1.0 mg/mL and 1 mM, respectively. (b) Without Cofactors (NADPH): 25 μL of 100 mM phosphate buffer was added to the incubations. The final concentration of microsomes was 1.0 mg/mL. The mixture was pre-warmed at 37 °C for 10 min. The reaction was started with the addition of 2.5 μL of 100 μM control compound or test compound solutions. Verapamil was used as positive control in this study. The final concentration of test compound or control compound was 1 μM. The incubation solution was incubated in water batch at 37 °C. Aliquots of 25 μL were taken from the reaction solution at 0.5, 5, 10, 15, 20, and 30 min. The reaction was stopped by the addition of five volumes of cold MeCN with IS (200 nM caffeine and 100 nM tolbutamide). Samples were centrifuged at 3,220 g for 40 min. An aliquot of 100 μL of the supernatant was mixed with 100 μL of ultrapure H_2O and then used for LC-MS/MS analysis. Verapamil (1 μM) was used as reference compounds, as unstable and stable compounds, respectively. *In vitro* scaled intrinsic clearance (CL_{int} scaled) was calculated from the half-life using the following equation

$$\textit{in vitro}\ CL_{int} = \left(\frac{0.693}{(t_{1/2})}\right) \times \left(\frac{\text{volume of incubation (μL)}}{\text{amount of proteins (mg)}}\right)$$

■ ASSOCIATED CONTENT

Supporting Information

The Supporting Information is available free of charge at https://pubs.acs.org/doi/10.1021/acs.jmedchem.1c01059.

^{1}H NMR and ^{13}C NMR spectra of representative compounds; binding to EED data (Figure S1); cell growth inhibition in KARPAS422 (Figure S2); crystallography data collection and refinement statistics (Table S1); difference electron density contoured to 3σ (Figure S3) (PDF)

Predicted_binding_model_compound_**10** (PDB)

Predicted_binding_model_compound_**22** (PDB)

Molecular string files for all of the final target compounds (CSV)

Accession Codes

Protein Data Bank codes are the following: compound **18**, 7MSB; compound **32**, 7MSD. The authors will release the atomic coordinates and experimental data upon article publication.

■ AUTHOR INFORMATION

Corresponding Author

Shaomeng Wang − *Rogel Cancer Center, Department of Internal Medicine, Department of Pharmacology, Medical School, and Department of Medicinal Chemistry, College of Pharmacy, University of Michigan, Ann Arbor, Michigan 48109, United States;* orcid.org/0000-0002-8782-6950; Email: shaomeng@umich.edu

Authors

Rohan Kalyan Rej − *Rogel Cancer Center and Department of Internal Medicine, University of Michigan, Ann Arbor, Michigan 48109, United States*

Changwei Wang − *Rogel Cancer Center and Department of Internal Medicine, University of Michigan, Ann Arbor, Michigan 48109, United States*

Jianfeng Lu − *Rogel Cancer Center and Department of Internal Medicine, University of Michigan, Ann Arbor, Michigan 48109, United States*

Mi Wang − *Rogel Cancer Center and Department of Internal Medicine, University of Michigan, Ann Arbor, Michigan 48109, United States*

Elyse Petrunak − *Department of Life Sciences Institute and Rogel Cancer Center, University of Michigan, Ann Arbor, Michigan 48109, United States*
Kaitlin P. Zawacki − *Rogel Cancer Center and Department of Internal Medicine, University of Michigan, Ann Arbor, Michigan 48109, United States*
Donna McEachern − *Rogel Cancer Center and Department of Internal Medicine, University of Michigan, Ann Arbor, Michigan 48109, United States*
Chao-Yie Yang − *Rogel Cancer Center and Department of Internal Medicine, University of Michigan, Ann Arbor, Michigan 48109, United States; Department of Pharmaceutical Sciences, College of Pharmacy, University of Tennessee Health Science Center, Memphis, Tennessee 38163, United States;* orcid.org/0000-0002-5445-0109
Lu Wang − *Department of Pharmaceutical Sciences, College of Pharmacy and Rogel Cancer Center, University of Michigan, Ann Arbor, Michigan 48109, United States*
Ruiting Li − *Department of Pharmaceutical Sciences, College of Pharmacy and Rogel Cancer Center, University of Michigan, Ann Arbor, Michigan 48109, United States*
Krishnapriya Chinnaswamy − *Department of Life Sciences Institute and Rogel Cancer Center, University of Michigan, Ann Arbor, Michigan 48109, United States*
Bo Wen − *Department of Pharmaceutical Sciences, College of Pharmacy, University of Michigan, Ann Arbor, Michigan 48109, United States*
Duxin Sun − *Department of Pharmaceutical Sciences, College of Pharmacy and Rogel Cancer Center, University of Michigan, Ann Arbor, Michigan 48109, United States;* orcid.org/0000-0002-6406-2126
Jeanne A. Stuckey − *Department of Life Sciences Institute and Rogel Cancer Center, University of Michigan, Ann Arbor, Michigan 48109, United States*
Yunlong Zhou − *Ascentage Pharma Group, Suzhou, Jiangsu 215216, China*
Jianyong Chen − *Ascentage Pharma Group, Suzhou, Jiangsu 215216, China*
Guozhi Tang − *Ascentage Pharma Group, Suzhou, Jiangsu 215216, China*

Complete contact information is available at: https://pubs.acs.org/10.1021/acs.jmedchem.1c01059

Author Contributions

◆R.K.R. and C.W. contributed equally

Notes

The authors declare the following competing financial interest(s): The University of Michigan has filed a patent application on these EED inhibitors, which has been licensed by Ascentage Pharma Group. S. Wang, R. Rej, C. Wang, M. Wang, J. Lu, C.-Y. Yang, E. Fernandez-Salas, and J. Stuckey are co-inventors on the patent application. The University of Michigan has received a research contract from Ascentage. S.W. is a co-founder of Ascentage, owns equity in Ascentage and is a paid consultant to Ascentage. The University of Michigan also owned equity in Ascentage.

■ ACKNOWLEDGMENTS

This work was supported in part by a research contract from Ascentage Pharma Group (to S.W.) and the Rogel Cancer Center Support Grant from National Cancer Institute, NIH (P30 CA046592). Use of the Advanced Photon Source, an Office of Science User Facility operated for the U.S. Department of Energy (DOE) Office of Science by Argonne National Laboratory, was supported by the U.S. DOE under Contract No. DE-AC02-06CH11357. Use of the LS-CAT Sector 21 was supported by the Michigan Economic Development Corporation and the Michigan Technology Tri-Corridor (Grant 085P1000817).

■ ABBREVIATIONS USED

PRC, polycomb repressive complex; EZH2, enhancer of zeste homolog 2; EED, embryonic ectoderm development; SUZ12, suppressor of zeste 12 protein homolog; H3K27, histone H3 lysine 27; SAM, S-adenosylmethionine; SAH, S-adenosyl-L-homocysteine hydrolase; NMR, nuclear magnetic resonance; DCM, dichloromethane; DMF, *N,N*-dimethylformamide; DMSO, dimethyl sulfoxide; DIPEA, *N,N*-diisopropylethylamine; HOAc, acetic acid; DCE, 1,2-dichloroethane; TFA, trifluoroacetic acid; HATU, 1-[bis(dimethylamino)-methylene]-1H-1,2,3-triazolo[4,5-*b*]-pyridinium 3-oxid hexafluorophosphate; SAR, structure−activity relationship; HPLC, high-performance liquid chromatography; PPA, polyphosphoric acid; rt, room temperature; UPLC, ultraperformance liquid chromatography; PK, pharmacokinetic; PO, per os; SCID mice, severe combined immunodeficiency mice; CL, volume of plasma cleared of the drug per unit time; SCID, severe combined immunodeficient; Vz, volume of distribution; Pd/C, palladium on carbon; LAH, lithium aluminum hydride; PPA, polyphosphoric acid

■ REFERENCES

(1) Simon, J. A.; Kingston, R. E. Mechanisms of Polycomb Gene Silencing: Knowns and Unknowns. *Nat. Rev. Mol. Cell Biol.* **2009**, *10*, 697−708.
(2) Levine, S. S.; Weiss, A.; Erdjument-Bromage, H.; Shao, Z.; Tempst, P.; Kingston, R. E. The Core of the Polycomb Repressive Complex Is Compositionally and Functionally Conserved in Flies and Humans. *Mol. Cell. Biol.* **2002**, *22*, 6070−6078.
(3) Dimou, A.; Dincman, T.; Evanno, E.; Gemmill, R. M.; Roche, J.; Drabkin, H. A. Epigenetics during EMT in Lung Cancer: EZH2 as a Potential Therapeutic Target. *Cancer Treat. Res. Commun.* **2017**, *12*, 40−48.
(4) Berdasco, M.; Esteller, M. Aberrant Epigenetic Landscape in Cancer: How Cellular Identity Goes Awry. *Dev. Cell* **2010**, *19*, 698−711.
(5) Martin, C.; Zhang, Y. The Diverse Functions of Histone Lysine Methylation. *Nat. Rev. Mol. Cell Biol.* **2005**, *6*, 838−849.
(6) Sato, T.; Kaneda, A.; Tsuji, S.; Isagawa, T.; Yamamoto, S.; Fujita, T.; Yamanaka, R.; Tanaka, Y.; Nukiwa, T.; Marquez, V. E.; Ishikawa, Y.; Ichinose, M.; Aburatani, H. PRC2 Overexpression and PRC2-Target Gene Repression Relating to Poorer Prognosis in Small Cell Lung Cancer. *Sci. Rep.* **2013**, *3*, No. 1911.
(7) Bödör, C.; O'Riain, C.; Wrench, D.; Matthews, J.; Iyengar, S.; Tayyib, H.; Calaminici, M.; Clear, A.; Iqbal, S.; Quentmeier, H.; Drexler, H. G.; Montoto, S.; Lister, A. T.; Gribben, J. G.; Matolcsy, A.; Fitzgibbon, J. EZH2 Y641 Mutations in Follicular Lymphoma. *Leukemia* **2011**, *25*, 726−729.
(8) Morin, R. D.; Johnson, N. A.; Severson, T. M.; Mungall, A. J.; An, J.; Goya, R.; Paul, J. E.; Boyle, M.; Woolcock, B. W.; Kuchenbauer, F.; Yap, D.; Humphries, R. K.; Griffith, O. L.; Shah, S.; Zhu, H.; Kimbara, M.; Shashkin, P.; Charlot, J. F.; Tcherpakov, M.; Corbett, R.; Tam, A.; Varhol, R.; Smailus, D.; Moksa, M.; Zhao, Y.; Delaney, A.; Qian, H.; Birol, I.; Schein, J.; Moore, R.; Holt, R.; Horsman, D. E.; Connors, J. M.; Jones, S.; Aparicio, S.; Hirst, M.; Gascoyne, R. D.; Marra, M. A. Somatic Mutations Altering EZH2 (Tyr641) in Follicular and Diffuse Large B-Cell Lymphomas of Germinal-Center Origin. *Nat. Genet.* **2010**, *42*, 181−185.

(9) Kim, K. H.; Roberts, C. W. M. Targeting EZH2 in Cancer. *Nat. Med.* **2016**, *22*, 128−134.
(10) Barsotti, A. M.; Ryskin, M.; Zhong, W.; Zhang, W. G.; Giannakou, A.; Loreth, C.; Diesl, V.; Follettie, M.; Golas, J.; Lee, M.; Nichols, T.; Fan, C.; Li, G.; Dann, S.; Fantin, V. R.; Arndt, K.; Verhelle, D.; Rollins, R. A. Epigenetic Reprogramming by Tumor-Derived EZH2 Gain-Offunction Mutations Promotes Aggressive 3D Cell Morphologies and Enhances Melanoma Tumor Growth. *Oncotarget* **2015**, *6*, 2928−2938.
(11) Yap, D. B.; Chu, J.; Berg, T.; Schapira, M.; Cheng, S. W. G.; Moradian, A.; Morin, R. D.; Mungall, A. J.; Meissner, B.; Boyle, M.; Marquez, V. E.; Marra, M. A.; Gascoyne, R. D.; Humphries, R. K.; Arrowsmith, C. H.; Morin, G. B.; Aparicio, S. A. J. R. Somatic Mutations at EZH2 Y641 Act Dominantly through a Mechanism of Selectively Altered PRC2 Catalytic Activity, to Increase H3K27 Trimethylation. *Blood* **2011**, *117*, 2451−2459.
(12) Garapaty-Rao, S.; Nasveschuk, C.; Gagnon, A.; Chan, E. Y.; Sandy, P.; Busby, J.; Balasubramanian, S.; Campbell, R.; Zhao, F.; Bergeron, L.; Audia, J. E.; Albrecht, B. K.; Harmange, J. C.; Cummings, R.; Trojer, P. Identification of EZH2 and EZH1 Small Molecule Inhibitors with Selective Impact on Diffuse Large B Cell Lymphoma Cell Growth. *Chem. Biol.* **2013**, *20*, 1329−1339.
(13) McCabe, M. T.; Ott, H. M.; Ganji, G.; Korenchuk, S.; Thompson, C.; Van Aller, G. S.; Liu, Y.; Pietra, A. D.; LaFrance, L. V.; Mellinger, M.; Duquenne, C.; Tian, X.; Kruger, R. G.; McHugh, C. F.; Miller, W. H.; Dhanak, D.; Verma, S. K.; Tummino, P. J.; Creasy, C. L.; Graves, A. P.; Diaz, E.; Brandt, M. EZH2 Inhibition as a Therapeutic Strategy for Lymphoma with EZH2-Activating Mutations. *Nature* **2012**, *492*, 108−112.
(14) Knutson, S. K.; Kawano, S.; Minoshima, Y.; Warholic, N. M.; Huang, K. C.; Xiao, Y.; Kadowaki, T.; Uesugi, M.; Kuznetsov, G.; Kumar, N.; Wigle, T. J.; Klaus, C. R.; Allain, C. J.; Raimondi, A.; Waters, N. J.; Smith, J. J.; Porter-Scott, M.; Chesworth, R.; Moyer, M. P.; Copeland, R. A.; Richon, V. M.; Uenaka, T.; Pollock, R. M.; Kuntz, K. W.; Yokoi, A.; Keilhack, H. Selective Inhibition of EZH2 by EPZ-6438 Leads to Potent Antitumor Activity in EZH2-Mutant Non-Hodgkin Lymphoma. *Mol. Cancer Ther.* **2014**, *13*, 842−854.
(15) Italiano, A.; Soria, J. C.; Toulmonde, M.; Michot, J. M.; Lucchesi, C.; Varga, A.; Coindre, J. M.; Blakemore, S. J.; Clawson, A.; Suttle, B.; McDonald, A. A.; Woodruff, M.; Ribich, S.; Hedrick, E.; Keilhack, H.; Thomson, B.; Owa, T.; Copeland, R. A.; Ho, P. T. C.; Ribrag, V. Tazemetostat, an EZH2 Inhibitor, in Relapsed or Refractory B-Cell Non-Hodgkin Lymphoma and Advanced Solid Tumours: A First-in-Human, Open-Label, Phase 1 Study. *Lancet Oncol.* **2018**, *19*, 649−659.
(16) Qi, W.; Zhao, K.; Gu, J.; Huang, Y.; Wang, Y.; Zhang, H.; Zhang, M.; Zhang, J.; Yu, Z.; Li, L.; Teng, L.; Chuai, S.; Zhang, C.; Zhao, M.; Chan, H.; Chen, Z.; Fang, D.; Fei, Q.; Feng, L.; Feng, L.; Gao, Y.; Ge, H.; Ge, X.; Li, G.; Lingel, A.; Lin, Y.; Liu, Y.; Luo, F.; Shi, M.; Wang, L.; Wang, Z.; Yu, Y.; Zeng, J.; Zeng, C.; Zhang, L.; Zhang, Q.; Zhou, S.; Oyang, C.; Atadja, P.; Li, E. An Allosteric PRC2 Inhibitor Targeting the H3K27me3 Binding Pocket of EED. *Nat. Chem. Biol.* **2017**, *13*, 381−388.
(17) He, Y.; Selvaraju, S.; Curtin, M. L.; Jakob, C. G.; Zhu, H.; Comess, K. M.; Shaw, B.; The, J.; Lima-Fernandes, E.; Szewczyk, M. M.; Cheng, D.; Klinge, K. L.; Li, H. Q.; Pliushchev, M.; Algire, M. A.; Maag, D.; Guo, J.; Dietrich, J.; Panchal, S. C.; Petros, A. M.; Sweis, R. F.; Torrent, M.; Bigelow, L. J.; Senisterra, G.; Li, F.; Kennedy, S.; Wu, Q.; Osterling, D. J.; Lindley, D. J.; Gao, W.; Galasinski, S.; Barsyte-Lovejoy, D.; Vedadi, M.; Buchanan, F. G.; Arrowsmith, C. H.; Chiang, G. G.; Sun, C.; Pappano, W. N. The EED Protein-Protein Interaction Inhibitor A-395 Inactivates the PRC2 Complex. *Nat. Chem. Biol.* **2017**, *13*, 389−395.
(18) Huang, Y.; Zhang, J.; Yu, Z.; Zhang, H.; Wang, Y.; Lingel, A.; Qi, W.; Gu, J.; Zhao, K.; Shultz, M. D.; Wang, L.; Fu, X.; Sun, Y.; Zhang, Q.; Jiang, X.; Zhang, J.; Zhang, C.; Li, L.; Zeng, J.; Feng, L.; Zhang, C.; Liu, Y.; Zhang, M.; Zhang, L.; Zhao, M.; Gao, Z.; Liu, X.; Fang, D.; Guo, H.; Mi, Y.; Gabriel, T.; Dillon, M. P.; Atadja, P.; Oyang, C. Discovery of First-in-Class, Potent, and Orally Bioavailable Embryonic Ectoderm Development (EED) Inhibitor with Robust Anticancer Efficacy. *J. Med. Chem.* **2017**, *60*, 2215−2226.
(19) Lingel, A.; Sendzik, M.; Huang, Y.; Shultz, M. D.; Cantwell, J.; Dillon, M. P.; Fu, X.; Fuller, J.; Gabriel, T.; Gu, J.; Jiang, X.; Li, L.; Liang, F.; McKenna, M.; Qi, W.; Rao, W.; Sheng, X.; Shu, W.; Sutton, J.; Taft, B.; Wang, L.; Zeng, J.; Zhang, H.; Zhang, M.; Zhao, K.; Lindvall, M.; Bussiere, D. E. Structure-Guided Design of EED Binders Allosterically Inhibiting the Epigenetic Polycomb Repressive Complex 2 (PRC2) Methyltransferase. *J. Med. Chem.* **2017**, *60*, 415−427.
(20) Curtin, M. L.; Pliushchev, M. A.; Li, H. Q.; Torrent, M.; Dietrich, J. D.; Jakob, C. G.; Zhu, H.; Zhao, H.; Wang, Y.; Ji, Z.; Clark, R. F.; Sarris, K. A.; Selvaraju, S.; Shaw, B.; Algire, M. A.; He, Y.; Richardson, P. L.; Sweis, R. F.; Sun, C.; Chiang, G. G.; Michaelides, M. R. SAR of Amino Pyrrolidines as Potent and Novel Protein-Protein Interaction Inhibitors of the PRC2 Complex through EED Binding. *Bioorg. Med. Chem. Lett.* **2017**, *27*, 1576−1583.
(21) Dong, H.; Liu, S.; Zhang, X.; Chen, S.; Kang, L.; Chen, Y.; Ma, S.; Fu, X.; Liu, Y.; Zhang, H.; Zou, B. An Allosteric PRC2 Inhibitor Targeting EED Suppresses Tumor Progression by Modulating the Immune Response. *Cancer Res.* **2019**, *79*, 5587−5596.
(22) Rej, R. K.; Wang, C.; Lu, J.; Wang, M.; Petrunak, E.; Zawacki, K. P.; McEachern, D.; Fernandez-Salas, E.; Yang, C. Y.; Wang, L.; Li, R.; Chinnaswamy, K.; Wen, B.; Sun, D.; Stuckey, J.; Zhou, Y.; Chen, J.; Tang, G.; Wang, S. EEDi-5285: An Exceptionally Potent, Efficacious, and Orally Active Small-Molecule Inhibitor of Embryonic Ectoderm Development. *J. Med. Chem.* **2020**, *63*, 7252−7267.
(23) Martin, M. C.; Zeng, G.; Yu, J.; Schiltz, G. E. Small Molecule Approaches for Targeting the Polycomb Repressive Complex 2 (PRC2) in Cancer. *J. Med. Chem.* **2020**, *63*, 15344−15370.
(24) Dockerill, M.; Gregson, C.; O' Donovan, D. H. Targeting PRC2 for the Treatment of Cancer: An Updated Patent Review (2016−2020). *Expert Opin. Ther. Pat.* **2021**, *31*, 119−136.
(25) Chang, C. E. A.; Chen, W.; Gilson, M. K. Ligand Configurational Entropy and Protein Binding. *Proc. Natl. Acad. Sci. U.S.A.* **2007**, *104*, 1534−1539.
(26) Fang, Z.; Song, Y.; Zhan, P.; Zhang, Q.; Liu, X. Conformational Restriction: An Effective Tactic in'Follow-on'-Based Drug Discovery. *Fut. Med. Chem.* **2014**, *6*, 885−901.
(27) Wang, S.; Rej, R.; Wang, C.; Wang, M.; Lu, J.; Yang, C.-Y.; Fernandez-Salas, E.; Stuckley, J. Preparation of Imidazopyrimidines as EED Inhibitors and the Use Thereof. WO2021/011713 A,2021; University of Michigan.
(28) Chan, H. M.; Fu, X.; Gu, X.-J. J.; Huang, Y.; Li, L.; Mi, Y.; Qi, W.; Sendzik, M.; Sun, Y.; Wang, L.; Yu, Z.; Zhang, H.; Zhang, J. Y. Jeff.; Zhang, M.; Zhang, Q.; Zhao, K. Imidazopyrimidine Compounds Useful for the Treatment of Cancer and Their Preparation. WO2017/221100 A2017; Novartis AG.
(29) Chan, H. M.; Fu, X.; Gu, X. J. J.; Huang, Y.; Li, L.; Mi, Y.; Qi, W.; Sendzik, M.; Sun, Y.; Wang, L.; Yu, Z.; Zhang, H.; Zhang, J. Y.; Zhang, M.; Zhang, Q.; Zhao, K. Triazolopyridine Compounds and Uses Thereof. WO2017221092A12017; Novartis AG.
(30) Xu, F.; Kim, J.; Waldman, J.; Wang, T.; Devine, P. Synthesis of Grazoprevir, a Potent NS3/4a Protease Inhibitor for the Treatment of Hepatitis C Virus. *Org. Lett.* **2018**, *20*, 7261−7265.
(31) Chemical Computing Group: Montreal, Quebec, Canada. Molecular Operating Environment (MOE).
(32) Verdonk, M. L.; Cole, J. C.; Hartshorn, M. J.; Murray, C. W.; Taylor, R. D. Improved Protein-Ligand Docking Using GOLD. *Proteins: Struct., Funct., Genet.* **2003**, *52*, 609−623.
(33) Jones, G.; Willett, P.; Glen, R. C.; Leach, A. R.; Taylor, R. Development and Validation of a Genetic Algorithm for Flexible Docking. *J. Mol. Biol.* **1997**, *267*, 727−748.
(34) Otwinowski, Z.; Minor, W. Processing of X-Ray Diffraction Data Collected in Oscillation Mode. *Methods Enzym.* **1997**, 307−326.
(35) Vagin, A.; Teplyakov, A. Molecular Replacement with MOLREP. *Acta Crystallogr., Sect. D: Biol. Crystallogr.* **2010**, *66*, 22−25.

https://doi.org/10.1021/acs.jmedchem.1c01059
J. Med. Chem. 2021, 64, 14540−14556

(36) Emsley, P.; Cowtan, K. Coot: Model-Building Tools for Molecular Graphics. *Acta Crystallogr., Sect. D: Biol. Crystallogr.* **2004**, *60*, 2126−2132.
(37) Roversi, P.; Sharff, A.; Smart, O. S.; Vonrhein, C.; Womack, T. O. *BUSTER*, version 2.11.2; Global Phasing Ltd.: Cambridge, United Kingdom, 2011.

https://doi.org/10.1021/acs.jmedchem.1c01059
J. Med. Chem. 2021, 64, 14540−14556